Retinal layer segmentation in multiple sclerosis: a systematic review and meta-analysis

*Axel Petzold, Laura J Balcer, Peter A Calabresi, Fiona Costello, Teresa C Frohman, Elliot M Frohman, Elena H Martinez-Lapiscina, Ari J Green, Randy Kardon, Olivier Outteryck, Friedemann Paul, Sven Schippling, Patrik Vermersch, Pablo Villoslada, Lisanne J Balk, on behalf of ERN-EYE and IMSVISUAL**

Summary

Background Structural retinal imaging biomarkers are important for early recognition and monitoring of inflammation and neurodegeneration in multiple sclerosis. With the introduction of spectral domain optical coherence tomography (SD-OCT), supervised automated segmentation of individual retinal layers is possible. We aimed to investigate which retinal layers show atrophy associated with neurodegeneration in multiple sclerosis when measured with SD-OCT.

Methods In this systematic review and meta-analysis, we searched for studies in which SD-OCT was used to look at the retina in people with multiple sclerosis with or without optic neuritis in PubMed, Web of Science, and Google Scholar between Nov 22, 1991, and April 19, 2016. Data were taken from cross-sectional cohorts and from one timepoint from longitudinal studies (at least 3 months after onset in studies of optic neuritis). We classified data on eyes into healthy controls, multiple-sclerosis-associated optic neuritis (MSON), and multiple sclerosis without optic neuritis (MSNON). We assessed thickness of the retinal layers and we rated individual layer segmentation performance by random effects meta-analysis for MSON eyes versus control eyes, MSNON eyes versus control eyes, and MSNON eyes versus MSON eyes. We excluded relevant sources of bias by funnel plots.

Findings Of 25 497 records identified, 110 articles were eligible and 40 reported data (in total 5776 eyes from patients with multiple sclerosis [1667 MSON eyes and 4109 MSNON eyes] and 1697 eyes from healthy controls) that met published OCT quality control criteria and were suitable for meta-analysis. Compared with control eyes, the peripapillary retinal nerve fibre layer (RNFL) showed thinning in MSON eyes (mean difference –20·10 µm, 95% CI –22·76 to –17·44; p<0·0001) and in MSNON eyes (–7·41 µm, –8·98 to –5·83; p<0·0001). The macula showed RNFL thinning of –6·18 µm (–8·07 to –4·28; p<0·0001) in MSON eyes and –2·15 µm (–3·15 to –1·15; p<0·0001) in MSNON eyes compared with control eyes. Atrophy of the macular ganglion cell layer and inner plexiform layer (GCIPL) was –16·42 µm (–19·23 to –13·60; p<0·0001) for MSON eyes and –6·31 µm (–7·75 to –4·87; p<0·0001) for MSNON eyes compared with control eyes. A small degree of inner nuclear layer (INL) thickening occurred in MSON eyes compared with control eyes (0·77 µm, 0·25 to 1·28; p=0·003). We found no statistical difference in the thickness of the combined outer nuclear layer and outer plexiform layer when we compared MSNON or MSON eyes with control eyes, but we found a small degree of thickening of the combined layer when we compared MSON eyes with MSNON eyes (1·21 µm, 0·24 to 2·19; p=0·01).

Interpretation The largest and most robust differences between the eyes of people with multiple sclerosis and control eyes were found in the peripapillary RNFL and macular GCIPL. Inflammatory disease activity might be captured by the INL. Because of the consistency, robustness, and large effect size, we recommend inclusion of the peripapillary RNFL and macular GCIPL for diagnosis, monitoring, and research.

Funding None.

Lancet Neurol 2017; 16: 797–812

See Comment page 764

*Members listed in appendix

Moorfields Eye Hospital, London, UK (A Petzold PhD); **Department of Neurology, Amsterdam Neuroscience, VUmc MS Center Amsterdam and Dutch Expertise Centre for Neuro-ophthalmology, VU University Medical Center, Amsterdam, Netherlands** (A Petzold, L J Balk PhD); **Institute of Neurology, University College London, London, UK** (A Petzold); **Department of Neurology, Department of Ophthalmology, and Department of Population Health, New York University School of Medicine, New York, NY, USA** (Prof L J Balcer MD); **Department of Neurology, Johns Hopkins Hospital, Baltimore, MD, USA** (Prof P A Calabresi MD); **Department of Clinical Neurosciences and Department of Surgery, University of Calgary, Calgary, AB, Canada** (Prof F Costello MD); **Department of Neurology, University of Texas Southwestern Medical Center, Dallas, TX, USA** (T C Frohman MD, Prof E M Frohman MD); **Center of Neuroimmunology, Institute of Biomedical Research August Pi Sunyer, Hospital Clinic of Barcelona, Barcelona, Spain** (E H Martinez-Lapiscina MD, Prof P Villoslada MD); **Multiple Sclerosis Center, Department of Neurology, University of California San Francisco, San Francisco, CA, USA** (Prof A J Green MD); **Iowa City VA Center for Prevention and Treatment of Visual Loss, Department of Veterans Affairs Hospital Iowa City, and Department of Ophthalmology and Visual Sciences, University of Iowa Hospital and Clinics, Iowa City, IA, USA** (Prof R Kardon MD); **Université**

Introduction

Optical coherence tomography (OCT) is a high-resolution imaging technique suitable for sophisticated post-processing.[1,2] Since our last meta-analysis,[3] use of time domain OCT (TD-OCT) has been overtaken by spectral domain OCT (SD-OCT) in clinical practice.[4] The much higher resolution of SD-OCT now permits analysis of individual retinal layer thicknesses.[5–8] This improvement in technique has enabled segmentation of ten additional retinal layers next to the well investigated retinal nerve fibre layer (RNFL).[9] Five of these layers have been analysed systematically in patients with multiple sclerosis: ganglion cell layer (GCL), inner plexiform layer (IPL), inner nuclear layer (INL), outer plexiform layer (OPL), and outer nuclear layer (ONL). In the present meta-analysis, we aimed to investigate what additional information can be derived by retinal layer segmentation in patients with multiple sclerosis and with optic neuritis associated with multiple sclerosis.

Methods

Search strategy and selection criteria

This study was a systematic review and meta-analysis of the thickness of individual retinal layers in multiple sclerosis. AP and LJBalk did the review of the Dutch, English, French, German, Italian, and Spanish literature on all studies (cross-sectional and longitudinal) with OCT in patients with multiple sclerosis published between the

Lille, CHRU Lille, LYRIC-INSERM U995, FHU Imminent, Lille, France (Prof P Vermersch MD); **Department of Neurology, University of Lille Nord de France, Lille, France** (O Outteryck MD); **NeuroCure Clinical Research Center, Charité, Department of Neurology, Experimental and Clinical Research Center, Max Delbrueck Center for Molecular Medicine and Charité Universitätsmedizin Berlin, Berlin, Germany** (Prof F Paul MD); **and Neuroimmunology and Multiple Sclerosis Research Section, University Hospital Zurich, Zurich, Switzerland** (Prof S Schippling MD)

Correspondence to:
Dr Axel Petzold, University College London, Institute of Neurology, London WC1N 3BG, UK
a.petzold@ucl.ac.uk

See Online for appendix

Research in context

Evidence before this study

A previous meta-analysis on retinal optical coherence tomography (OCT) in multiple sclerosis considered all evidence since invention of the method in 1991. All data were based on time domain OCT (TD-OCT). The main finding (exactly the same as for our study) was that evidence was consistent for atrophy of the peripapillary retinal nerve fibre layer (RNFL). Data from the TD-OCT studies on individual retinal layers were scarce because of poor image resolution and an absence of segmentation algorithms. With the event of spectral domain OCT (SD-OCT), both limitations can be overcome. A new body of literature now exists on quantitative individual retinal layer OCT data. For this new meta-analysis, we considered all published evidence on these new SD-OCT data in multiple sclerosis. We used PubMed, Web of Science, and Google Scholar, and searches were done in six languages by authors fluent in Dutch, English, French, German, Italian, and Spanish. The first search terms were "optical coherence tomography" and the names of the SD-OCT devices on the market. We refined the list of articles by searching for "multiple sclerosis", "demyelination", "optic neuritis", and the abbreviations "MS", "CIS", "RRMS", "SPMS", "PPMS", "ON", and "MSON". We reviewed the methods section of the identified articles to find out which of the studies did indeed use the SD-OCT methods. We assessed the quality of the studies with the Advised Protocol for OCT Study Terminology and Elements (APOSTEL) recommendations for studies on quantitative OCT.

Added value of this study

New data were available on individual retinal layers, which allowed for detailed analysis of the macula, in addition to the peripapillary region studied in the previous meta-analysis. Each of these two areas had retinal-layer-specific anatomical advantages, with the RNFL being thickest at the optic disc and the ganglion cell layer thickest in the macula. Our evidence shows that the macula has a similar degree of atrophy to that previously shown for the peripapillary RNFL. The results also show that atrophy of retinal layers in multiple sclerosis stops at the inner nuclear layer. Consequently, volume changes of the inner nuclear layer have emerged as a potentially new surrogate for inflammation-related changes in multiple sclerosis. We report new evidence for an increase of outer nuclear layer volume following optic neuritis. New longitudinal evidence for a disease duration-dependent degree of inner retinal layer (RNFL and ganglion cell layer and inner plexiform layer [GCIPL]) atrophy, which is most marked in the early disease course.

Implications of all the available evidence

The meta-analysis shows that SD-OCT provides a reproducible, accurate, and robust method for quantification of individual retinal layers. The data imply a need to routinely (in clinical practice, research, and trials) undertake OCT scans from two different regions per eye: the optic disc and the macular. Particularly in clinical practice, these two scans would help with the differential diagnosis and with identification of macular pathology. The data further suggest outcome measures that could be prioritised in studies of multiple sclerosis. For atrophy, these are the peripapillary RNFL and the macular GCIPL, and for inflammation, this is probably the inner nuclear layer.

first report of the method by Huang and colleagues[1] on Nov 22, 1991, and April 19, 2016, including manuscripts published ahead of print. We searched PubMed, Web of Science, and Google Scholar with a hierarchical search strategy. We searched for OCT, including the brand and device names of the major commercial suppliers, and then we refined this search using the following search terms: multiple sclerosis, demyelination, optic neuritis, and the abbreviations "MS", "CIS", "RRMS", "SPMS", "PPMS", "ON", and "MSON". We reviewed articles for use of SD-OCT. Diagnosis of multiple sclerosis and multiple-sclerosis-associated optic neuritis (MSON) were defined as per consensus.[10–13] We excluded articles if they did not contain patients with multiple sclerosis, included fewer than ten participants, did not use SD-OCT, did not separate eyes with optic neuritis in patients who had multiple sclerosis (MSON eyes) from eyes in patients who had multiple sclerosis without optic neuritis (MSNON eyes), were communications in response to an article, were duplications of data already published from the same cohort, or reported data in a format other than mean (SD) or mean (SEM; study authors were contacted and asked to supply this information). Articles that did not contain a group of control patients were excluded if they did not contain data permitting comparison of MSON eyes with the MSNON eyes. Conflicts on inclusion of data were resolved by consensus (between AP and LJBalk).

Data analysis

AP and LJBalk independently extracted data. Extracted data consisted of mean thickness (SD) of individual retinal layers (RNFL, GCL, IPL, a combination of GCL and IPL, INL, ONL, OPL, or a combination of ONL and OPL) of eyes of patients with multiple sclerosis (with and without a history of MSON) and healthy control participants. Because of the anatomical structure of the retina (appendix), data were reported for the RNFL at the optic disc and macula, but for all other layers only at the macula. To solve conflicts of inclusion for the meta-analysis, authors of the research papers were approached by email regarding inclusion criteria, timing of events, and presentation of data (mean, SD, and number). Key papers excluded from the meta-analysis because of unsuitable or duplicate data were still referenced in the systematic review. No grey

literature sources were assessed and we used only summary estimates. The main outcome measure was thickness (μm) of peripapillary RNFL and macular RNFL, GCL, IPL, GCL and IPL combined (GCIPL), INL, and ONL and OPL combined (ONPL) in MSON eyes, MSNON eyes, and healthy control eyes. We reported results as mean difference (μm, with 95% CI) between the MSON eyes, MSNON eyes, and control eyes for all retinal layers. We assessed variability within studies (sampling error) and between studies with the I^2 estimate of heterogeneity. Retinal OCT data for different SD-OCT devices were analysed together. Data were taken from cross-sectional studies and from one single timepoint from longitudinal studies. The baseline OCT values were taken from longitudinal studies that did not include acute optic neuritis. Because the time lag between onset of MSON and ensuing retinal layer atrophy, follow-up data were taken from these studies from one single timepoint, which had to be at least 3 months after onset of MSON.[14] No subgroup analyses according to disease course were done if they would have led to loss of power and because the new classification into active and stable disease by Lublin and colleagues[15] has not yet been applied systematically. Data on individual retinal layer thickness were entered for each group of eyes as mean thickness in μm (SD) to compare the predefined groups for MSON eyes, MSNON eyes, and eyes of healthy control participants. Categorisation of the groups was done at the eye level, instead of at the patient level. For OCT research-specific quality assessment we used the Advised Protocol for OCT Study Terminology and Elements (APOSTEL) recommendations,[9] which are based on validated OCT quality control criteria.[16,17] We considered p values of 0·05 or less as significant. We assessed publication bias with funnel plots.

The analyses of SD-OCT were identical in design to our previous meta-analysis[3] on TD-OCT, to enable comparison of the data. We used Review Manager (RevMan) version 5.3 following the guidance of the Diagnostic Test Accuracy Working Group.[18] Retinal layer thickness data were entered as a continuous variable. We used inverse variance, with random effects (DerSimonian and Laird). We chose random effects instead of a fixed effects analysis because of the level of heterogeneity between studies reported previously[3] and because different OCT devices and segmentation algorithms were used in the studies. On an individual patient level the devices and algorithms are not directly comparable.[19] On a group level the degree of atrophy can still be extracted, but study heterogeneity will increase. We have therefore labelled data derived by different OCT manufacturers in our forest plots.

We summarised the results of the meta-analyses for related retinal layers. For each layer, subgroup analyses are presented for the comparison of MSON eyes with control eyes, then for the comparison of MSNON eyes with control eyes, and finally, for the comparison of MSON eyes with MSNON eyes.

Role of the funding source

There was no funding source for this study. The corresponding author had full access to all the data in the study and had final responsibility for the decision to submit for publication.

Results

Figure 1 summarises the selection process for the 110 articles that reported SD-OCT in multiple sclerosis (the appendix has the full list of references). Of these, 40 articles[6,14,20–57] presented data suitable (in five cases after contacting the authors for additional information [stated as not estimable when data were not provided]) for meta-analysis of retinal layer thickness between groups (table).

Atrophy of the peripapillary RNFL and macular RNFL occurred in MSON eyes compared with control eyes (figure 2A) and MSNON eyes compared with control eyes (figure 2B). When comparing the eyes of patients

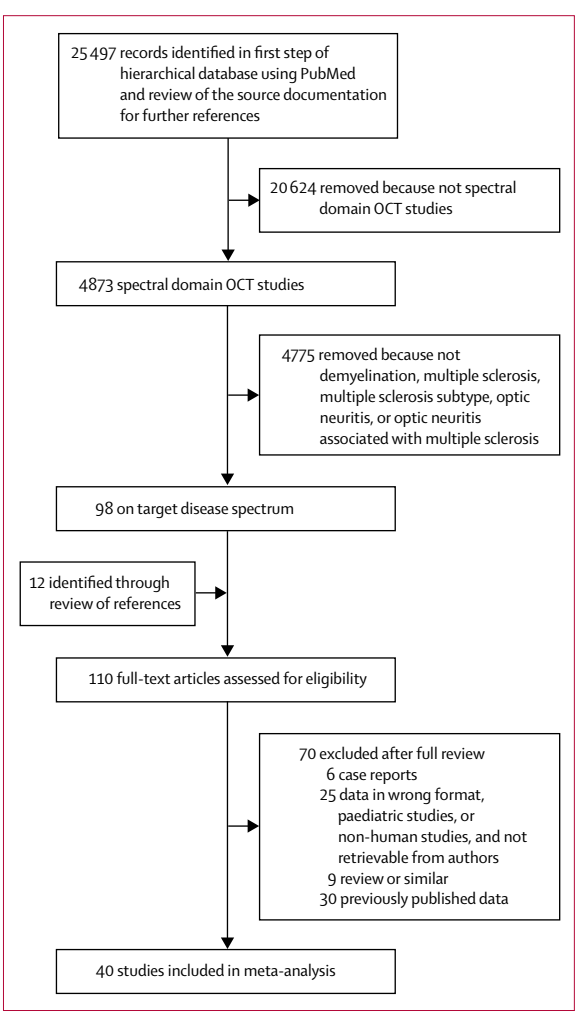

Figure 1: **Study selection**

	Women (%)	Age (years)	EDSS score	Disease duration*	Multiple sclerosis criteria	Optic neuritis criteria	MSNON (n)†	MSON (n)†	Control (n)	OCT device
Al-Louzi et al (2016)[20]	88% in multiple sclerosis group; no data for control group	36 (9)	NA	7 (3–11) years	McDonald 2010	In-house	33	33	NA	Cirrus (Carl Zeiss Meditec)
Balk et al (2014)[21]	68% in multiple sclerosis group and 65% in control group	54 (10) in multiple sclerosis group and 51 (7) in control group	4 (1–8)	20 (7) years	McDonald 2005	Not specified	230	106	63	Spectralis (Heidelberg Engineering)
Behbehani et al (2015)[22]	64% in multiple sclerosis group and 65% in control group	30 (9) in multiple sclerosis group and 30 (6) in control group	2·21 (1·34)	37 (9) months	McDonald 2010	Not specified	104	32	51	3D OCT 2000 (Topcon Corporation)
Behbehani et al (2016)[23]	60% in multiple sclerosis group and 40% in control group	27 (2) in multiple sclerosis group and 29 (5) in control group	NA	14 (11) days	Not applicable	Not specified	NA	10	10	Cirrus (Carl Zeiss Meditec)
Chilinska et al (2016)[24]	58% in multiple sclerosis group and 58%‡ in control group	45 (21–72) in multiple sclerosis group; no data provided for control group	Mean 4·5 (2–6·5)	13 (4–39) years	McDonald§	Not specified	59	34 (eyes)	28	Spectralis (Heidelberg Engineering)
Costello et al (2015)[14]	84% in multiple sclerosis group; no control group	36 (9) in multiple sclerosis group	NA	29 months (34)	Not specified	In-house¶	19	50	NA	Cirrus (Carl Zeiss Meditec)
Esen et al (2016)[25]	66% in multiple sclerosis group and 67% in control group	40 (9) in multiple sclerosis group and 39 (8) in control group	Mean 2·1 (0–5·5)	92 months (64)	McDonald 2010	In-house	47	27	30	Cirrus (Carl Zeiss Meditec)
Feng et al (2013)[26]	50% in optic neuritis group and 36% in non-optic neuritis group	44 (16) in optic neuritis group and 31 (9) in non-optic neuritis group	NA	83 months (82) in optic neuritis group and 61 months (74) in non-optic neuritis group	McDonald 2010	Not specified	28	16	NA	Cirrus (Carl Zeiss Meditec)
Fernandes et al (2013)[27]	87% in MSON group, 86% in MSNON group, and 78% in control group‖	34·3 (8·7) in MSON group, 35·3 (10·2) in MSNON group, and 36·0 (12·5) in control group	NA	5 years (1–26) in MSON group and 3 years (1–21) in MSNON group	McDonald 2001	In-house	29	44	45	3D OCT-2000 (Topcon Corporation)
Fjeldstad et al (2011)[28]	NA	42 (2) in multiple sclerosis group and 33 (3) in control group	NA	NA	McDonald 2001	Not applicable	30	NA	60	Cirrus (Carl Zeiss Meditec)
Garcia-Martin et al (2013)[29]	67% in multiple sclerosis group and 67% in control group	42 (10) in multiple sclerosis group and 42 (11) in control group	Mean 2·45 (0–8)	9·2 years (0·5–39)	McDonald 2001	In-house	106	31 (eyes)	115	Spectralis (Heidelberg Engineering)
Gelfand et al (2012)[30]	80% in CIS group, 72% in RRMS group, 68% in SPMS group, 45% in PPMS group, and 57% in control group	39 (10) in CIS group, 42 (11) in RRMS group, 51 (11) in SPMS group, 52 (12) in PPMS group, and 35 (11) in control group	1·5 (1–2) in CIS group, 2 (1·5–3·5) in RRMS group, 5·5 (4–6·5) in SPMS group, 5·5 (4–6·5) in PPMS group	1 year (0–3) in CIS group, 7 years (3–12) in RRMS group, 14 years (6–21) in SPMS group, and 9 years (4–12) in PPMS group	McDonald 2005	In-house	541	262 (eyes)	60	Spectralis (Heidelberg Engineering)
González-López et al (2014)[31]	63% in multiple sclerosis group and 57% in control group	40 (10) in multiple sclerosis group and 37 (10) in control group	Mean 2·4 (1·7)	6·8 years (7)	McDonald 2005	In-house	36 (eyes)	104 (eyes)	70	Cirrus (Carl Zeiss Meditec)
Hadhoum et al (2015)[32]	61% in multiple sclerosis group; no control group	34 (19–54)	2 (0–6)	86 months (6–237)	Not specified	Petzold et al (2014)[11]	25	25	NA	Spectralis (Heidelberg Engineering)**
Hokazono et al (2013)[33]	86% in multiple sclerosis group and 100% in control group	36·8 (11·5) in multiple sclerosis group and 36·0 (12·5) in control group	NA	5 years (1–26)	McDonald 2010	In-house	22 (eyes)	29 (eyes)	26	3D OCT-1000 (Topcon Corporation)

(Table continues on next page)

	Women (%)	Age (years)	EDSS score	Disease duration*	Multiple sclerosis criteria	Optic neuritis criteria	MSNON (n)†	MSON (n)†	Control (n)	OCT device
(Continued from previous page)										
Huang-Link et al (2015)[34]	72% in multiple sclerosis group and 73% in control group	44 (12) in multiple sclerosis group and 40 (14) in control group	1 (0–5)	11 years (0·5–38)	McDonald 2005	In-house	36	12	34	Cirrus (Carl Zeiss Meditec)
Kaushik et al (2013)[35]	78% in multiple sclerosis group and 75% in control group	39·5 (9·8) in multiple sclerosis group and 39·5 (10·7) in control group	NA	Mean 52 months (range 3–178)	McDonald 2001	In-house	0	36	36	Spectralis (Heidelberg Engineering)
Khalil et al (2016)[36]	79% in multiple sclerosis group and 83% in control group	34 (8) in multiple sclerosis group and 36 (9) in control group	4·9 (1·7)	7 years (6)	McDonald 2005	Voss et al (2011)[12]	68	30 (eyes)	23	RTVue (Optovue Inc)
Khanifar et al (2010)[37]	68% in multiple sclerosis group	39 (26–69)	NA	Median 31 months (range NA)	Not specified	In-house	47	25 (eyes)	NA	Spectralis (Heidelberg Engineering)
Klistorner et al (2014)[38]	74% in multiple sclerosis group and control group were sex-matched	40·2 (11·6) in multiple sclerosis group years and control group were age-matched	NA	4·8 years (3·1)	Not specified	In-house	53	0	50	Spectralis (Heidelberg Engineering)
Knier et al (2016)[39]	76% in multiple sclerosis group and 59% in control group	52·8 (8·8) in multiple sclerosis group and 49·0 (10·2) in control group	2·5 (1·0–3·0)	24·9 years (7·2)	Poser 1965 or McDonald 2005	In-house	25 (eyes)	33 (eyes)	29	Spectralis (Heidelberg Engineering)
Lange et al (2013)[40]	92% in multiple sclerosis group and 88% in control group	44 (9) in multiple sclerosis group and 49 (10) in control group	2·5 (1–6·5)	12 years (8)	McDonald 2005	Not specified	25	20	50	Spectralis (Heidelberg Engineering)
Modvig et al (2016)[41]	83% in control group; not provided for multiple sclerosis group	33 in control group	NA	NA	Not specified	In-house	47††	43 (eyes)‡‡	30	Cirrus (Carl Zeiss Meditec)
Narayanan et al (2014)[42]	76·7% in multiple sclerosis group	43·4 (11·1)	NA	8·5 years (8·0)	McDonald 2005	Becket al[13]	149	98	0	Cirrus (Carl Zeiss Meditec)
Oberwahrenbrock et al (2012)[43]	66% in multiple sclerosis group and 67% in control group	41 (10) in multiple sclerosis group and 35 (10) in control group	2 (0–8)	107 months (90)	McDonald 2005	Not specified	414	183 (eyes)	94	Spectralis (Heidelberg Engineering)
Oberwahrenbrock et al (2013)[6]	69% in multiple sclerosis group and 69% in control group	32 (8) in multiple sclerosis group and 32 (8) in control group	1 (0–4)	NA	McDonald 2010	In-house	45	16	45	Spectralis (Heidelberg Engineering)
Park et al (2014)[44]	73% in multiple sclerosis group and 66% in control group	32 (3) in multiple sclerosis group and 41 (12) in control group	NA	2 years (0·6)	McDonald 2005	Not specified	15	15	24	Spectralis (Heidelberg Engineering)
Petracca et al (2016)[45]	56% in multiple sclerosis group and 56% in control group	52 (32–65) in multiple sclerosis group and 51 (34–63) in control group	4 (1·5–6)	9 years (5)	McDonald 2010	Not applicable	25	0	20	Spectralis (Heidelberg Engineering)
Rebolleda, et al (2011)[46]	68% in multiple sclerosis group	Median 39 (range NA)	NA	Median 2·5 years (range NA)	Not specified	In-house	18 (eyes)§§	18	NA	Cirrus (Carl Zeiss Meditec)¶¶
Saidha et al (2015)[47]	75% in multiple sclerosis group	44·2 (12·1)	Median 3 (IQR 2–6)	Median 10 years (IQR 4–16)	McDonald 2010	In-house	60 (eyes)	154 (eyes)	0	Cirrus (Carl Zeiss Meditec)
Salari et al (2015)[48]	92% in multiple sclerosis group	27 (5)	NA	NA	McDonald 2010	In-house	52	52 (eyes)‖‖	NA	3D OCT-1000 (Topcon Corporation)
Schneider et al (2013)[49]	94% in multiple sclerosis group and 94% in control group	41 (13) in multiple sclerosis group and 41 (12) in control group	NA	65 months (36)	McDonald 2010	In-house	17	20 (eyes)	17	Spectralis (Heidelberg Engineering)

(Table continues on next page)

	Women (%)	Age (years)	EDSS score	Disease duration*	Multiple sclerosis criteria	Optic neuritis criteria	MSNON (n)†	MSON (n)†	Control (n)	OCT device
(Continued from previous page)										
Schnurman et al (2014)[50]	78% in multiple sclerosis group and not specified in control group	44 (9) in multiple sclerosis group and 31 (11) in control group	2·7 (1–6·5)	8·9 years (5·8)	McDonald 2010	In-house	18	18	18	Spectralis (Heidelberg Engineering)
Soufi et al (2015)[51]	81% in multiple sclerosis group and 26% in control group	37 (10) in multiple sclerosis group and 31 (7) in control group	3·2 (2·2)	5 years (2–7)	McDonald 2010	Not specified	31	7	31	3D OCT-2000 (Topcon Corporation)
Sriram et al (2014)[52]	69% in multiple sclerosis group and 69% in control group	Age-matched (not further specified)	NA	4·7 years (2·9)	Not specified	In-house	58	0	25	Spectralis (Heidelberg Engineering)
Sriram et al (2012)[53]	60% in multiple sclerosis group and 61% in control group	37 (9) in multiple sclerosis group and 37 (10) in control group	NA	3·7 years (0·8)	McDonald 2001	In-house	15	15	18	Spectralis (Heidelberg Engineering)
Syc et al (2012)[54]	71% in multiple sclerosis group and 70% in control group	42 (10) in multiple sclerosis group and 41 (8) in control group	NA	12 years (9)	Not specified	In-house	98	20	50	Cirrus (Carl Zeiss Meditec)
Walter et al (2012)[55]	65% in multiple sclerosis group and 66% in control group	43 (14) in multiple sclerosis group and 37 (10) in control group	2 (0–8·5)	9 years (11)	McDonald 2005	In-house	213	52	47	Spectralis (Heidelberg Engineering)
Xu et al (2016)[56]	75% in multiple sclerosis group 71% in control group	45 in multiple sclerosis group*** and 41 in control group	NA	11 years	McDonald 2010	In-house	76	30	24	Cirrus (Carl Zeiss Meditec)
Zimmermann et al (2013)[57]	73% in multiple sclerosis group	41 (9) in multiple sclerosis group	2 (0–6)	79 months (58)	McDonald 2005	In-house	77 (eyes)	46 (eyes)	NA	Cirrus (Carl Zeiss Meditec)

Data are presented as %, mean (SD), median (range), n, or as stated. EDSS score and disease duration are presented only for patients with multiple sclerosis, because neither variable was applied to control individuals. Diagnostic criteria were indicated as in-house when authors provided information permitting to make the diagnosis. We refer the reader to the original work for more details about interpretation of individual assessments. The SD-OCT devices used were from Heidelberg Engineering (Heidelberg, Germany), Carl Zeiss Meditec (Dublin, CA, USA), Optovue Inc (Fremont, CA, USA), and Topcon Corporation (Tokyo, Japan). EDSS=Expanded Disability Status Scale. MSNON=multiple sclerosis without optic neuritis. MSON=multiple-sclerosis-associated optic neuritis. OCT=optical coherence tomography. NA=data not available. CIS=clinically isolated syndrome. RRMS=relapsing-remitting multiple sclerosis. SPMS=secondary-progressive multiple sclerosis. PPMS=primary-progressive multiple sclerosis. TD-OCT=time domain optical coherence tomography. SD-OCT=spectral domain optical coherence tomography. *Disease duration at baseline is presented for longitudinal studies. †Number of patients and not eyes with MSON is given, unless specified otherwise. ‡Paper states that controls were age-matched and sex-matched to multiple sclerosis cohort. §Year of revision of the McDonald criteria used not further specified. ¶Patients with a first clinical presentation of unilateral optic neuritis who underwent clinical evaluation within 1 month of symptom onset were included in the study. ||Numbers in table[27] do not add up to 29 participants with MSON, of which four patients were male and 26 patients were female. The male to female ratio was taken for calculation of percentage in this table. The same discrepency occurred for MSNON. **This paper reported the volume rather than the thickness (device-dependent) explaining the numbers in figures 3, 4. ††Data refer to 47 (84%) of 56 patients included originally from a previous publication. ‡‡OCT data from 46 MSON eyes at baseline and 43 MSON eyes at follow-up. §§Data on 18 MSON eyes and 18 fellow MSNON eyes. ¶¶Study also used TD-OCT (Stratus), but only SD-OCT data were included in the meta-analysis. ||||SD-OCT data were taken from 52 MSON eyes at 6 months' follow-up. ***Weighted average calculated for age and disease duration.

Table: **Characteristics of studies included in the meta-analysis**

with multiple sclerosis, the atrophy in MSON eyes was greater than that in MSNON eyes (figure 2C). No publication bias was shown (appendix).

The meta-analysis for the GCIPL showed atrophy in the MSON eyes compared with control eyes (figure 3A). In MSNON eyes, we found atrophy of the GCIPL compared with control eyes (figure 3B). For the eyes of patients with multiple sclerosis, atrophy of the GCL and IPL was more marked in MSON eyes than in MSNON eyes (figure 3C). No publication bias was shown (appendix).

For the INL, the mean difference between the MSON eyes and control eyes indicated thickening of the INL (figure 4A). The INL remained unchanged in MSNON eyes compared with control eyes (figure 4B). When comparing the eyes of patients with multiple sclerosis, a thickened INL was observed in MSON eyes compared with MSNON eyes and the average thickening was small (figure 4C). No publication bias was shown (appendix).

The meta-analysis for the ONPL showed that no change in thickness occurred in MSON eyes or MSNON eyes compared with control eyes (figure 4D, E). The ONPL seemed to be slightly thickened in MSON eyes compared with MSNON eyes (figure 4F). No publication bias was shown (appendix).

Overall, the largest effect sizes for comparisons between groups were seen for the peripapillary RNFL and GCIPL (figure 5). The effects sizes were small for the INL (significant only when comparing MSON eyes with other eyes) and ONPL (significant only when comparing MSON with MSNON eyes).

A

	Device	MSON		Control		Weight (%)	Mean difference* (μm; 95% CI)
		Mean (μm; SD)	Total eyes	Mean (μm; SD)	Total eyes		
Peripapillary RNFL							
Balk et al (2014)[21]	H	76·4 (11·6)	144	91·7 (6·8)	126	7·3	−15·30 (−17·54 to −13·06)
Behbehani et al (2015)[22]	T	101·3 (14·4)	32	111·3 (8·7)	51	5·8	−10·00 (−15·53 to −4·47)
Behbehani et al (2016)[23]	Z	82 (14·1)	10	94·9 (6)	40	4·1	−12·90 (−21·83 to −3·97)
Esen et al (2016)[25]	Z	82·2 (11·8)	40	96·7 (8·2)	60	6·5	−14·50 (−18·70 to −10·30)
Feng et al (2013)[26]	Z	71·8 (19·2)	12	102·1 (8·1)	28	3·2	−30·30 (−41·57 to −19·03)
Gelfand et al (2012)[30]	H	80·2 (17·8)	262	101·3 (10·1)	106	7·1	−21·10 (−23·99 to −18·21)
Gonzalez-Lopez et al (2014)[31]	Z	79·6 (13·6)	36	99·3 (8·7)	140	6·2	−19·70 (−24·37 to −15·03)
Huang-Link et al (2015)[34]	Z	67·7 (7·91)	15	93·6 (8·9)	68	6·3	−25·90 (−30·43 to −21·37)
Khalil et al (2016)[36]	O	84·1 (13·5)	30	117·8 (26·2)	23	3·1	−33·70 (−45·45 to −21·95)
Lange et al (2013)[40]	H	73·9 (15·2)	13	98·4 (8·8)	100	4·3	−24·50 (−32·94 to −16·06)
Oberwahrenbrock et al (2012)[43]	H	77·8 (14·6)	183	100·6 (8·8)	183	7·2	−22·80 (−25·27 to −20·33)
Oberwahrenbrock et al (2013)[6]	H	82·1 (18)	16	101·4 (7·4)	90	4·1	−19·30 (−28·25 to −10·35)
Park et al (2014)[44]	H	70·1 (6)	15	100·1 (9·3)	24	6·2	−30·00 (−34·80 to −25·20)
Rebolleda et al (2011)[46]	Z	81 (0)	18	93·5 (0)	18	..	Not estimable
Schneider et al (2013)[49]	H	85·3 (13·3)	20	100·1 (10·8)	34	5·1	−14·80 (−21·67 to −7·93)
Soufi et al (2015)[51]	T	77 (11)	7	104 (8·7)	58	4·3	−27·00 (−35·45 to −18·55)
Syc et al (2012)[54]	Z	78·7 (11·7)	73	93·4 (10·4)	100	6·9	−14·70 (−18·07 to −11·33)
Walter et al (2012)[55]	H	78·4 (13·6)	87	92·9 (9·9)	61	6·7	−14·50 (−18·29 to −10·71)
Xu et al (2016)[56]	Z	73·6 (14·8)	35	97·1 (11·5)	41	5·5	−23·50 (−29·54 to −17·46)
Total (N)			**1030**		**1333**	**100·0**	**−20·10 (−22·76 to −17·44)**
Heterogeneity: τ^2=23·83; χ^2=97·35, df=17 (p<0·0001); I^2=83%							
Test for overall effect: Z=14·82 (p<0·0001)							
Macular RNFL							
Balk et al (2014)[21]	H	24 (2·9)	114	27·3 (2·1)	126	17·9	−3·30 (−3·95 to −2·65)
Fernandes et al (2013)[27]	T	30·6 (9·4)	45	37·9 (5·4)	82	12·6	−7·30 (−10·28 to −4·32)
Hokazono et al (2013)[33]	T	30·1 (8·7)	29	39 (5)	30	10·9	−8·90 (−12·54 to −5·26)
Kaushik et al (2013)[35]	H	27·8 (4)	36	32·2 (2)	36	16·5	−4·40 (−5·86 to −2·94)
Oberwahrenbrock et al (2013)[6]	H	32·1 (5·6)	16	39·9 (4·6)	90	12·8	−7·80 (−10·70 to −4·90)
Schneider et al 2013)[49]	H	29·4 (4)	20	33·4 (2·3)	34	15·4	−4·00 (−5·92 to −2·08)
Walter et al (2012)[55]	H	19·9 (9)	87	29·6 (6)	61	14·1	−9·70 (−12·12 to −7·28)
Total (95% CI)			**347**		**459**	**100·0**	**−6·18 (−8·07 to −4·28)**
Heterogeneity: τ^2=5·12; χ^2=97·35, df=6 (p<0·0001); I^2=86%							
Test for overall effect: Z=6·39 (p<0·0001)							

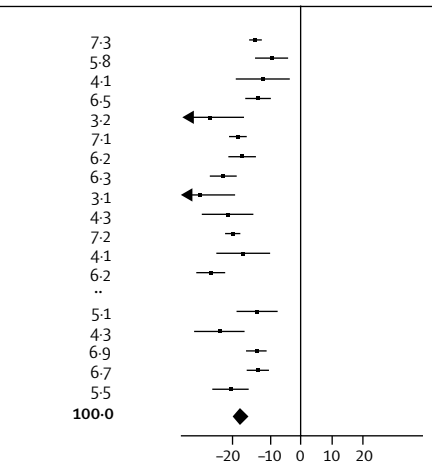

B

	Device	MSNON		Control		Weight (%)	Mean difference* (μm; 95% CI)
		Mean (μm; SD)	Total eyes	Mean (μm; SD)	Total eyes		
Peripapillary RNFL							
Balk et al (2014)[21]	H	85·5 (10·1)	279	91·7 (6·8)	126	8·2	−6·20 (−7·88 to −4·52)
Behbehani et al (2015)[22]	T	102·7 (11·5)	72	111·3 (8·7)	51	6·1	−8·60 (−12·17 to −5·03)
Behbehani et al (2016)[23]	Z	89 (16·2)	10	94·9 (6)	40	1·9	−5·90 (−16·11 to 4·31)
Esen et al (2016)[25]	Z	89·2 (11·2)	54	96·7 (8·2)	60	6·1	−7·50 (−11·14 to −3·86)
Feng et al (2013)[26]	Z	92 (8·5)	12	102·1 (8·1)	28	4·2	−10·10 (−15·77 to −4·43)
Fjeldstad et al (2011)[28]	Z	89·1 (0)	60	98 (0)	32	..	Not estimable
Garcia-Martin et al (2013)[29]	H	93 (0)	75	99·5 (8·9)	115	..	Not estimable
Gelfand et al (2012)[30]	H	91·5 (13·7)	820	101·3 (10·1)	106	7·7	−9·80 (−11·94 to −7·66)
Gonzalez-Lopez et al (2014)[31]	Z	90·7 (12·7)	104	99·3 (8·7)	140	7·0	−8·60 (−11·43 to −5·77)
Huang-Link et al (2015)[34]	Z	87·7 (9·7)	15	93·6 (8·9)	68	4·4	−5·90 (−11·25 to −0·55)
Khalil et al (2016)[36]	O	92·4 (17·7)	38	117·8 (26·2)	23	1·4	−25·40 (−37·50 to −13·30)
Klistorner et al (2014)[38]	H	94 (6·5)	53	99 (9·8)	50	6·5	−5·00 (−8·23 to −1·77)
Knier et al (2016)[39]	H	97 (10·4)	36	100·1 (8·6)	38	5·3	−3·10 (−7·46 to 1·26)
Lange et al (2013)[40]	H	93·2 (14·4)	37	98·4 (8·8)	100	4·8	−5·20 (−10·15 to −0·25)
Oberwahrenbrock et al (2012)[43]	H	90·2 (12·3)	571	100·6 (9·4)	183	8·1	−10·40 (−12·09 to −8·71)
Oberwahrenbrock et al (2013)[6]	H	99·9 (11·3)	66	100·7 (8)	66	6·4	−0·80 (−4·14 to 2·54)
Petracca et al (2016)[45]	H	86·9 (13·6)	50	92·8 (12·4)	40	4·4	−5·90 (−11·28 to −0·52)
Soufi et al (2015)[51]	T	91 (11)	55	104 (8·7)	58	6·0	−13·00 (−16·67 to −9·33)
Walter et al (2012)[55]	H	87·6 (11·1)	150	92·9 (9·9)	61	6·7	−5·30 (−8·35 to −2·25)
Xu et al (2016)[56]	Z	89·3 (11·5)	41	97·1 (11·5)	41	4·7	−7·80 (−12·78 to −2·82)
Total (95% CI)			**2463**		**1279**	**100·0**	**−7·41 (−8·98 to −5·83)**
Heterogeneity: τ^2=7·21; χ^2=61·78, df=17 (p<0·0001); I^2=72%							
Test for overall effect: Z=9·20 (p<0·0001)							
Macular RNFL							
Balk et al (2014)[21]	H	26·1 (2·7)	279	27·3 (2·1)	126	27·6	−1·20 (−1·68 to −0·72)
Fernandes et al (2013)[27]	T	35·5 (6)	74	37·9 (5·4)	82	15·1	−2·40 (−4·20 to −0·60)
Hokazono et al (2013)[33]	T	35·7 (5·8)	22	39 (5)	30	8·0	−3·30 (−6·31 to −0·29)
Knier et al (2016)[39]	H	29·2 (4·1)	36	32 (3·7)	38	15·2	−2·80 (−4·58 to −1·02)
Oberwahrenbrock et al (2013)[6]	H	38·8 (3)	66	39·7 (4·5)	66	19·6	−0·90 (−2·20 to 0·40)
Walter et al (2012)[55]	H	25·5 (7·1)	150	29·6 (6)	61	14·4	−4·10 (−5·99 to −2·21)
Total (95% CI)			**627**		**403**	**100·0**	**−2·15 (−3·15 to −1·15)**
Heterogeneity: τ^2=0·88; χ^2=13·96, df=5 (p=0·02); I^2=64%							
Test for overall effect: Z=4·22 (p<0·0001)							

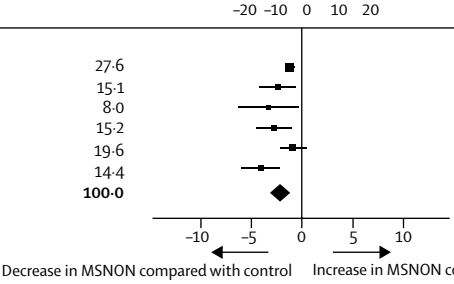

(Figure 2 continues on next page)

C

	Device	MSON		MSNON		Weight (%)	Mean difference* (µm; 95% CI)
		Mean (µm; SD)	Total eyes	Mean (µm; SD)	Total eyes		
Peripapillary RNFL							
Al-Louzi et al (2015)[20]	Z	82·1 (14·9)	9	92·8 (9·8)	16	2·0	−10·70 (−21·55 to 0·15)
Balk et al (2014)[21]	H	76·4 (11·6)	144	85·5 (10·1)	279	7·9	−9·10 (−11·33 to −6·87)
Behbehani et al (2015)[22]	T	101·3 (14·4)	32	102·7 (11·5)	72	4·7	−1·40 (−7·05 to 4·25)
Chilinska et al (2015)[24]	H	79·6 (32·7)	34	88·9 (30)	73	1·5	−9·30 (−22·27 to 3·67)
Costello et al (2015)[15]	Z	75·3 (13·7)	50	90·4 (14·3)	50	4·8	−15·10 (−20·59 to −9·61)
Esen et al (2016)[25]	Z	82·2 (11·8)	40	89·2 (11·2)	45	5·3	−7·00 (−11·91 to −2·09)
Feng et al (2013)[26]	Z	71·8 (19·2)	12	92 (8·5)	12	1·8	−20·20 (−32·08 to −8·32)
Gelfand et al (2012)[30]	H	80·2 (17·8)	262	91·5 (13·7)	820	7·8	−11·30 (−13·65 to −8·95)
Gonzalez-Lopez et al (2014)[31]	H	79·6 (13·6)	36	90·7 (12·7)	104	5·2	−11·10 (−16·17 to −6·03)
Hadhoum et al (2015)[22]	Z	74·2 (19·9)	50	94·9 (10·8)	20	3·5	−20·70 (−27·97 to −13·43)
Huang-Link et al (2015)[34]	H	67·7 (7·91)	15	87·7 (9·7)	57	5·5	−20·00 (−24·73 to −15·27)
Khalil et al (2016)[36]	Z	84·1 (13·5)	30	92·4 (17·7)	38	3·5	−8·30 (−15·72 to −0·88)
Khanifar et al (2010)[37]	O	83 (14)	25	90·5 (13·2)	69	4·2	−7·50 (−13·81 to −1·19)
Lange et al (2013)[40]	H	73·9 (15·2)	13	93·2 (14·4)	37	2·5	−19·30 (−28·78 to −9·82)
Modvig et al (2015)[41]	H	71·5 (0)	43	95·5 (0)	40	..	Not estimable
Oberwahrenbrock et al (2012)[43]	Z	77·8 (14·6)	183	90·2 (8·5)	571	8·0	−12·40 (−14·63 to −10·17)
Saidha et al (2015)[47]	H	76·5 (10·4)	60	86·9 (11·4)	130	6·9	−10·40 (−13·68 to −7·12)
Salari et al (2015)[48]	Z	96·1 (12·3)	52	104·4 (9·5)	52	6·0	−8·30 (−12·52 to −4·08)
Schnurman et al (2014)[50]	T	72·7 (18·7)	33	90·2 (10·6)	25	3·3	−17·50 (−25·11 to −9·89)
Soufi et al (2015)[51]	H	77 (11)	7	91 (11)	55	2·8	−14·00 (−22·65 to −5·35)
Walter et al (2012)[55]	T	78·4 (13·6)	87	87·6 (11·1)	150	6·8	−9·20 (−12·56 to −5·84)
Zimmermann et al (2013)[57]	H	82 (12)	46	90 (10)	77	6·1	−8·00 (−12·12 to −3·88)
Total (95% CI)	Z		**1220**		**2752**	**100·0**	**−11·25 (−13·00 to −9·50)**
Heterogeneity: τ^2=8·72; χ^2=55·90, df=20 (p<0·0001); I^2=64%							
Test for overall effect: Z=12·61 (p<0·0001)							
Macular RNFL							
Balk et al (2014)[21]	H	24 (2·9)	114	26·1 (2·7)	279	47·9	−2·10 (−2·72 to −1·48)
Fernandes et al (2013)[27]	T	30·6 (9·4)	45	35·5 (6)	74	27·5	−4·90 (−7·97 to −1·83)
Hadhoum et al (2015)[22]	H	0 (0)	50	0 (0)	20	..	Not estimable
Hokazono et al (2013)[33]	T	30·1 (8·7)	29	35·5 (6)	74	24·6	−5·40 (−8·85 to −1·95)
Total (95% CI)			**188**		**427**	**100·0**	**−3·68 (−6·10 to −1·27)**
Heterogeneity: τ^2=3·07; χ^2=6·26, df=2 (p=0·04); I^2=68%							
Test for overall effect: Z=2·99 (p=0·003)							

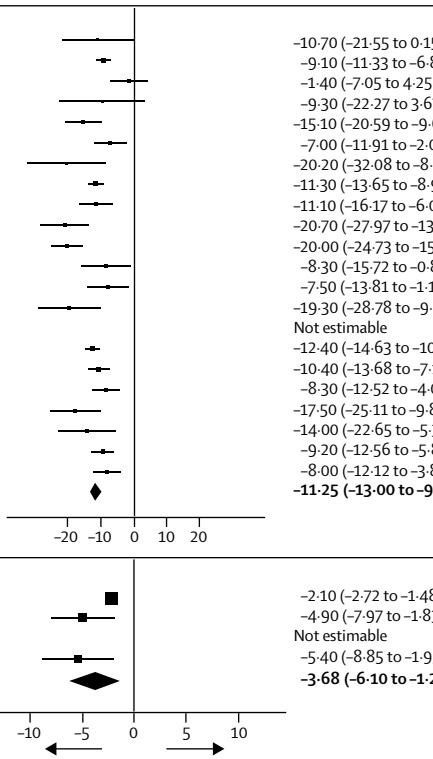

***Figure 2*: Meta-analysis of peripapillary RNFL and macular RNFL SD-OCT data**

RNFL data from MSON eyes (A) or MSNON eyes (B) compared with control eyes, and a comparison between MSON eyes and MSNON eyes (C). Horizontal bars indicate 95% CI. Numbers in the total row exclude eyes for which a mean difference was not estimable. The four SD-OCT devices used are indicated as H (Spectralis, Heidelberg Engineering; Heidelberg, Germany), Z (Cirrus, Carl Zeiss Meditec; Dublin, CA, USA), O (RTVue, Optovue Inc; Fremont, CA, USA), and T (3D OCT-2000, Topcon Corporation; Tokyo, Japan). The appendix shows the corresponding funnel plots. RNFL=retinal nerve fibre layer. SD-OCT=spectral domain optical coherence tomography. MSON eyes=eyes with multiple-sclerosis-associated optic neuritis. MSNON eyes=eyes without multiple sclerosis optic neuritis. *Inverse variance with random effects.

Discussion

In this meta-analysis, the data suggest that multiple sclerosis is associated with atrophy of retinal ganglion cells (GCL and GCIPL) and their axons (peripapillary RNFL and macular RNFL). Importantly, the effect sizes shown for the meta-analysis based on SD-OCT of the peripapillary RNFL almost exactly matched the effect sizes from our meta-analysis[3] based on TD-OCT. This outcome emphasises the robustness and accuracy of the peripapillary RNFL as a measure for neurodegeneration in multiple sclerosis and optic neuritis associated with multiple sclerosis, spanning two generations of OCT-device technology. Although the new meta-analysis is comprehensive and provides a valuable summary of available data on the thickness of all retinal layers from peripapillary RNFL to ONL in patients with multiple sclerosis, it should be noted that this meta-analysis is based on solely observational studies, which are not without limitations.[58,59]

It was not possible to accurately resolve individual layers of the macula with TD-OCT.[3,60] Our study shows that using SD-OCT, the macular RNFL, GCL or GCIPL, INL, and ONL or ONPL can now be reliably quantified with data suitable for meta-analysis. These new quantitative layer segmentation data extend earlier peripapillary RNFL data by showing that inner retinal layer atrophy is severe after optic neuritis associated with multiple sclerosis, but still prominent in the eyes of patients with multiple sclerosis who never had optic neuritis compared with control eyes. Interpretation of the quantitative statistical data cannot be extrapolated to individual patients for small retinal layer thickness changes because the axial resolution of SD-OCT devices used in clinical routine is about 3–7 µm. On a group level, different segmentation algorithms and different generations of OCT technology deliver comparable data. This result is consistent with an earlier head-to-head comparison of OCT devices in patients with multiple sclerosis.[61]

In human vision the first-order, second-order, and third-order neurons and their axons are hardwired

projections of the human brain and transmit analogue and digital signals.[62] This hardwired single pathway enables the retinotopic map of the human visual cortex.[63] Anatomically the GCL, macular RNFL, and peripapillary RNFL represent the first unit within this pathway. Axonotmesis (irreversible axonal damage) at any point in this pathway is understood to give rise to retrograde trans-synaptic axonal degeneration, which will inexorably cause atrophy of the inner retinal layers' atrophy (RNFL and GCIPL).[64] Trans-synaptic degeneration affects the dorsal lateral geniculate nucleus, but stops at the INL (appendix). The INL contains the first bipolar neuron of this hardwired pathway and acts as a physiological barrier to retrograde trans-synaptic degeneration. This feature renders the INL an attractive layer for investigation of inflammation (thickening; figure 5).

Six studies[42,47,65–68] reported longitudinal data. With TD-OCT, Talman and colleagues[67] reported an annual atrophy rate of –1·4 µm/year in 381 patients with multiple sclerosis, which was closely matched by the SD-OCT data (–1·49 µm/year, n=96) from Narayanan and colleagues.[42] Later studies found the annual peripapillary RNFL atrophy rate to be about a third of that in the earlier studies, with an average of –0·36 µm/year (n=107),[47] –0·5 µm/year (n=45),[66] and –0·53 µm/year (n=168).[65] One study[68] (n=58) found no significant changes over a 2-year period.

The differences in annual atrophy rates might partly be explained by differences in the demographic data. The

A

	Device	MSON		Control		Weight (%)	Mean difference* (µm; 95% CI)
		Mean (µm; SD)	Total eyes	Mean (µm; SD)	Total eyes		
GCIPL							
Balk et al (2014)[21]†	H	70·5 (17·3)	144	94·2 (6)	126	6·5	–23·70 (–26·71 to –20·69)
Behbehani et al (2016)[23]	Z	67·8 (9·6)	10	84·1 (3·5)	40	5·3	–16·30 (–22·35 to –10·25)
Esen et al (2016)[25]	Z	69·2 (9·3)	40	85·9 (4·6)	60	6·5	–16·70 (–19·81 to –13·59)
Fernandes et al (2013)[27]	T	61·7 (10·1)	45	70·3 (7·2)	82	6·4	–8·60 (–11·94 to –5·26)
Gonzalez-Lopez et al (2014)[31]	Z	66·4 (10·9)	36	83·8 (5·9)	140	6·3	–17·40 (–21·09 to –13·71)
Hokazono et al (2013)[33]	T	59·3 (8·7)	29	70·3 (5·6)	30	6·2	–11·00 (–14·75 to –7·25)
Huang-Link et al (2015)[34]	Z	61·5 (5·9)	15	82 (5·1)	68	6·4	–20·50 (–23·72 to –17·28)
Kaushik et al (2013)[35]	H	69·3 (14)	36	98·1 (5)	36	5·8	–28·80 (–33·66 to –23·94)
Khalil et al (2016)[36]	O	84·3 (11·9)	30	96·2 (21)	23	3·9	–11·90 (–21·48 to –2·32)
Oberwahrenbrock et al (2013)[6]	H	58·7 (9·8)	16	71·6 (4·6)	90	5·8	–12·90 (–17·80 to –8·00)
Park et al (2014)[44]	H	37·2 (9·8)	15	53·6 (19·3)	24	4·0	–16·40 (–25·58 to –7·22)
Schneider et al (2013)[49]†	H	36·1 (5·8)	20	45·5 (5·1)	34	6·5	–9·40 (–12·47 to –6·33)
Soufi et al (2015)[51]	T	55·7 (7·4)	7	73·5 (6·7)	58	5·4	–17·80 (–23·55 to –12·05)
Sriram et al (2012)[53]	H	58·7 (7·4)	15	81·8 (12·5)	34	5·5	–23·10 (–28·73 to –17·47)
Syc et al (2012)[54]	Z	65·6 (10·4)	73	81·9 (6·5)	100	6·6	–16·30 (–19·00 to –13·60)
Walter et al (2012)[55]	H	79·7 (9·1)	87	88·9 (6·9)	61	6·6	–9·20 (–11·78 to –6·62)
Xu et al (2016)[56]	Z	63·6 (9·1)	35	83 (5·6)	41	6·3	–19·40 (–22·87 to –15·93)
Total (95% CI)			**653**		**1047**	**100·0**	**–16·42 (–19·23 to –13·60)**

Heterogeneity: τ^2=29·36; χ^2=1·4243, df=16 (p<0·0001); I^2=89%
Test for overall effect: Z=11·44 (p<0·0001)

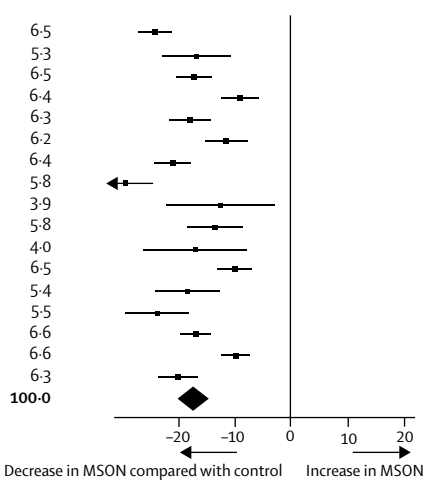

B

	Device	MSNON		Control		Weight (%)	Mean difference* (µm; 95% CI)
		Mean (µm; SD)	Total eyes	Mean (µm; SD)	Total eyes		
GCIPL							
Balk et al (2014)[21]†	H	84·2 (13·1)	279	94·2 (6)	126	6·8	–10·00 (–11·86 to –8·14)
Behbehani et al (2016)[23]	Z	76·7 (10·9)	10	84·1 (3·5)	40	2·8	–7·40 (–14·24 to –0·56)
Esen et al (2016)[25]	Z	76·8 (8·8)	54	85·9 (4·6)	60	6·1	–9·10 (–11·72 to –6·48)
Fernandes et al (2013)[27]	T	64·4 (6·9)	74	70·3 (7·2)	82	6·5	–5·90 (–8·11 to –3·69)
Gonzalez-Lopez et al (2014)[31]	Z	74·3 (10·7)	104	83·8 (5·9)	140	6·4	–9·50 (–11·78 to –7·22)
Hokazono et al (2013)[33]	T	64·5 (7·2)	22	70·3 (5·6)	30	5·2	–5·80 (–9·41 to –2·19)
Huang-Link et al (2015)[34]	Z	76·8 (8)	57	82 (5·1)	68	6·3	–5·20 (–7·60 to –2·80)
Khalil et al (2016)[36]	O	86·3 (13·8)	38	96·2 (21)	23	1·7	–9·90 (–19·54 to –0·26)
Klistorner et al (2014)[38]	H	81·8 (7)	53	87·3 (4)	50	6·5	–5·50 (–7·69 to –3·31)
Knier et al (2016)[39]	H	70 (6·7)	36	71·5 (5)	38	6·0	–1·50 (–4·21 to 1·21)
Oberwahrenbrock et al (2013)[6]	H	68·9 (5·5)	66	71·3 (4·5)	66	6·9	–2·40 (–4·11 to –0·69)
Petracca et al (2016)[45]	H	66 (9·4)	50	72·6 (6·7)	40	5·4	–6·60 (–9·93 to –3·27)
Soufi et al (2015)[51]	T	66·2 (9·6)	55	73·5 (6·7)	58	5·7	–7·30 (–10·37 to –4·23)
Sriram et al (2012)[53]	H	72·6 (11·2)	15	81·8 (12·5)	34	2·7	–9·20 (–16·26 to –2·14)
Sriram et al (2014)[52]	H	81·4 (7·1)	58	86·5 (5·5)	25	5·9	–5·10 (–7·93 to –2·27)
Syc et al (2012)[54]	Z	73·2 (9·3)	123	81·9 (6·5)	100	6·6	–8·70 (–10·78 to –6·62)
Walter et al (2012)[55]	H	86·8 (6·6)	150	88·9 (6·9)	61	6·7	–2·10 (–4·13 to –0·07)
Xu et al (2016)[56]	Z	75·6 (8·4)	41	83 (5·6)	41	5·7	–7·40 (–10·49 to –4·31)
Total (95% CI)			**1285**		**1082**	**100·0**	**–6·31 (–7·75 to –4·87)**

Heterogeneity: τ^2=7·00; χ^2=84·63, df=17 (p<0·0001); I^2=80%
Test for overall effect: Z=8·61 (p<0·0001)

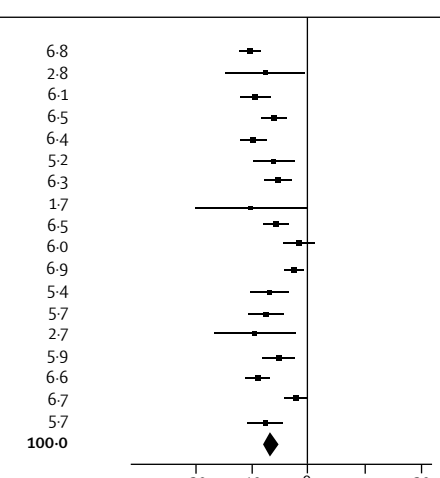

(Figure 3 continues on next page)

C

	Device	MSON		MSNON			Mean difference* (μm; 95% CI)
		Mean (μm; SD)	Total eyes	Mean (μm; SD)	Total eyes		
GCIPL							
Al-Louzi et al (2015)[20]	Z	68·8 (10·8)	9	78·4 (6·3)	16	3·1	−9·60 (−17·30 to −1·90)
Balk et al (2014)[21]†	H	70·5 (17·3)	144	84·2 (13·1)	279	6·4	−13·70 (−16·92 to −10·48)
Costello et al (2015)[14]†	Z	64·6 (9)	50	77·9 (9·4)	50	6·1	−13·30 (−16·91 to −9·69)
Esen et al (2016)[25]	Z	69·2 (9·3)	40	76·8 (8·8)	54	6·0	−7·60 (−11·32 to −3·88)
Fernandes et al (2013)[27]	T	61·7 (10·1)	45	64·4 (6·9)	74	6·3	−2·70 (−6·04 to 0·64)
Gonzalez-Lopez et al (2014)[31]	Z	66·4 (10·9)	36	74·3 (10·7)	104	5·6	−7·90 (−12·01 to −3·79)
Hadhoum et al (2015)[22]†	H	0 (0)	50	0 (0)	20	5·4	Not estimable
Hokazono et al (2013)[33]	T	59·3 (8·7)	29	64·5 (7·2)	22	6·0	−5·20 (−9·57 to −0·83)
Huang-Link et al (2015)[34]	Z	61·5 (5·9)	15	76·8 (8)	57	4·0	−15·30 (−18·94 to −11·66)
Khalil et al (2016)[36]	O	84·3 (11·9)	30	86·3 (13·8)	38	6·8	−2·00 (−8·11 to 4·11)
Modvig et al (2015)[41]	Z	63 (0)	43	83 (0)	40	4·8	Not estimable
Narayanan et al (2014)[42]	Z	65·5 (11·9)	98	76·5 (9·8)	149	6·8	−11·00 (−13·83 to −8·17)
Oberwahrenbrock et al (2013)[6]	H	58·7 (9·8)	16	68·9 (5·5)	66	4·0	−10·20 (−15·18 to −5·22)
Saidha et al (2015)[47]	Z	63·9 (9·3)	60	73·5 (8·9)	130	2·9	−9·60 (−12·41 to −6·79)
Schnurman et al (2014)[50]	H	0 (0)	33	0 (0)	25	6·7	Not estimable
Soufi et al (2015)[51]	T	55·7 (7·4)	7	66·2 (9·6)	55	7·3	−10·50 (−16·54 to −4·46)
Sriram et al (2012)[53]	H	72·6 (11·2)	15	72·6 (11·2)	15	5·4	0·00 (−8·02 to 8·02)
Syc et al (2012)[54]	Z	65·6 (10·4)	73	73·2 (9·3)	123	6·4	−7·60 (−10·50 to −4·70)
Walter et al (2012)[55]	H	79·7 (9·1)	87	86·8 (6·6)	150		−7·10 (−9·28 to −4·92)
Xu et al (2016)[56]	Z	63·6 (9·1)	35	75·2 (7·9)	25		−11·60 (−15·92 to −7·28)
Zimmermann et al (2013)[57]	Z	70 (10)	46	78 (7)	77		−8·00 (−11·29 to −4·71)
Total (95% CI)			**835**		**1484**	**100·0**	**−8·81 (−10·50 to −7·12)**

Heterogeneity: τ^2=8·92; χ^2=60·53, df=17 (p<0·0001); I^2=72%
Test for overall effect: Z=10·20 (p<0·0001)

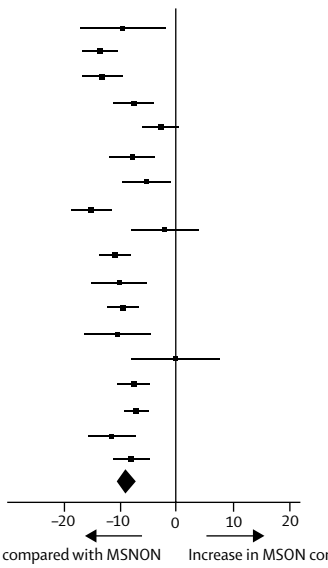

Figure 3: **Meta-analysis of macular GCIPL SD-OCT data**

GCIPL data from MSON eyes (A) or MSNON eyes (B) compared with control eyes, and a comparison between MSON eyes and MSNON eyes (C). Horizontal bar indicates 95% CI. Numbers in the total row exclude eyes for which a mean difference was not estimable. The four SD-OCT devices used are indicated as H (Spectralis, Heidelberg Engineering; Heidelberg, Germany), Z (Cirrus, Carl Zeiss Meditec; Dublin, CA, USA), O (RTVue, Optovue Inc; Fremont, CA, USA), and T (3D OCT-2000, Topcon Corporation; Tokyo, Japan). The appendix shows the corresponding funnel plots. GCIPL=ganglion cell layer and inner plexiform layer. SD-OCT=spectral domain optical coherence tomography. MSON eyes=eyes with multiple-sclerosis-associated optic neuritis. MSNON eyes=eyes without multiple sclerosis optic neuritis. *Inverse variance with random effects. †All studies measured ganglion cell layer (GCL) and inner plexiform layer (IPL) thickness combined (GCIPL) because of the poor image contrast between GCL and IPL, except as indicated in which studies only measured GCL thickness.

highest annual atrophy rate was found in patients with multiple sclerosis who did not have optic neuritis and those who had a shorter disease duration.[65] A plateau effect was observed in patients with a longer disease duration (>20 years).[65] Likewise, annual atrophy rate was higher in MSON eyes (–0·91 μm/year) compared with MSNON eyes (–0·53 μm/year).[66] But this outcome was opposite to what Narayanan and colleagues[42] had reported, with a lower annual atrophy rate in MSON eyes (–1·27 μm/year) than in MSNON eyes (–1·49 μm/year).

A conservative estimate from these data is that, with a 1 μm loss every 1–2 years with an OCT-device accuracy threshold of about 2–3 μm, a clinical trial of 2–3 years with patients with active disease[15] would be powered for probing potential neuroprotection against peripapillary RNFL atrophy. During the early disease course a shorter trial duration might be sufficient.[65] Mechanisms that could be a good target in trials with the peripapillary RNFL as an outcome measure are inflammatory disease activity in multiple sclerosis[69–71] and non-demyelinating mechanisms, such as mitochondrial dysfunction.[72,73] SD-OCT segmentation has been used as an outcome marker in a trial investigating potential remyelination,[74] published in 2017.

A limitation of peripapillary RNFL data that is not directly evident from the meta-analyses is caused by optic disc swelling at presentation.[75] The longitudinal study by Kupersmith and colleagues[75] shows superiority of the GCIPL compared with the peripapillary RNFL for detection of early atrophy following optic neuritis. Nonetheless, the mean atrophy of the peripapillary RNFL following MSON was 20·38 μm (95% CI 17·91–22·86) for TD-OCT data[3] and 20·10 μm (17·44–22·76) in our SD-OCT data. In MSNON eyes, mean atrophy of the peripapillary RNFL was 7·08 μm (5·52–8·65) for TD-OCT data[3] and 7·41 μm (5·83–8·98) in our SD-OCT data. Finally, comparison of MSON eyes and MSNON eyes showed averaged peripapillary RNFL atrophy of 13·84 μm (11·72–15·97) for TD-OCT data[3] and 11·25 μm (9·50–13·00) in our SD-OCT data. The almost identical findings for TD-OCT and SD-OCT data highlight that the peripapillary RNFL is well suited for use as an outcome measure in clinical trials. Achievement of no evident disease activity with disease-modifying treatment in multiple sclerosis has been associated with less marked atrophy of the peripapillary RNFL longitudinally.[69]

Consistent with the data from the RNFL, atrophy of the GCL and IPL was more severe in MSON eyes than in MSNON eyes. An important advantage of the GCIPL compared with the peripapillary RNFL is that atrophy becomes detectable much earlier.[75,76] At 1 month after optic neuritis associated with multiple sclerosis, thinning of the GCIPL becomes quantifiable compared with baseline values, while for the peripapillary RNFL the advice is to wait at least 3 months.[5,11] Reassuringly, this

finding is corroborated by a different meta-analysis,[77] which also included neuromyelitis optica. Additionally, the retinal ganglion cell layer complex is the thickest in the macula. Because this layer has a large dynamic range and most of the multiple sclerosis-related damage, in CNS and the retina, includes the macula, it seems that the GCIPL is a good biomarker for neurodegeneration in the visual pathway. In cases with severe atrophy of the peripapillary RNFL following optic neuritis associated with multiple sclerosis, a floor effect might prevent observation of further atrophy around the optic disc, but analysis of the GCIPL will still be useful.

No atrophy was observed for the INL. By contrast, the thickening of this layer was more substantial in MSON eyes than in MSNON eyes. An association of INL thickening with inflammatory activity has also been reported previously.[69,70] Importantly, longitudinal data showed that INL microcysts were mostly (>80%) transient (dynamic).[78,79] A transient increase of INL thickness might be a sign of retinal inflammation or failure to maintain retinal fluid homoeostasis,[80] consistent with the original description of microcystic macular oedema in multiple sclerosis.[81] Several independent lines of evidence suggest the existence of a retinal glymphatic system with a

A

	Device	MSON		Control		Weight (%)	Mean difference* (µm; 95% CI)
		Mean (µm; SD)	Total eyes	Mean (µm; SD)	Total eyes		
INL							
Balk et al (2014)[21]	H	42·3 (3)	144	41·4 (2·9)	126	27·3	0·90 (0·20 to 1·60)
Fernandes et al (2013)[27]	T	31·4 (2·7)	45	31·4 (2·7)	82	18·4	0·00 (–0·98 to 0·98)
Hokazono et al (2013)[33]	T	31·7 (2·5)	29	31·2 (1·7)	30	15·8	0·50 (–0·59 to 1·59)
Kaushik et al (2013)[35]	H	42·9 (6)	36	39·6 (3)	36	5·0	3·30 (1·11 to 5·49)
Oberwahrenbrock et al (2013)[6]	H	34·9 (2·2)	16	34·3 (2·4)	90	14·0	0·60 (–0·59 to 1·79)
Schneider et al (2013)[49]	H	39·3 (3·1)	20	38·9 (3·1)	34	7·7	0·40 (–1·31 to 2·11)
Sriram et al (2012)[53]	H	43·5 (4·2)	15	42·7 (4·7)	34	3·5	0·80 (–1·85 to 3·45)
Walter et al (2012)[55]	H	45 (5·6)	87	43·4 (4·5)	61	8·4	1·60 (–0·03 to 3·23)
Total (95% CI)			**392**		**493**	**100·0**	**0·77 (0·25 to 1·28)**

Heterogeneity: τ^2=0·12; χ^2=9·08 to df=7 (p=0·25); I^2=23%
Test for overall effect: Z=2·93 (p=0·003)

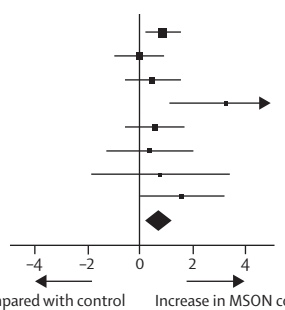

B

	Device	MSNON		Control		Weight (%)	Mean difference* (µm; 95% CI)
		Mean (µm; SD)	Total eyes	Mean (µm; SD)	Total eyes		
INL							
Balk et al (2014)[21]	H	41·5 (3)	279	41·4 (2·9)	126	18·7	0·10 (–0·52 to 0·72)
Fernandes et al (2013)[27]	T	31 (2·6)	74	31·4 (2·7)	82	15·5	–0·40 (–1·23 to 0·43)
Hokazono et al (2013)[33]	T	31·7 (2·5)	22	31·2 (1·7)	30	10·9	0·50 (–0·71 to 1·71)
Klistorner et al (2014)[38]	H	37·7 (3·2)	53	37·1 (2·9)	50	11·2	0·60 (–0·58 to 1·78)
Knier et al (2016)[39]	H	35·4 (1·8)	36	34 (2·2)	38	14·4	1·40 (0·49 to 2·31)
Oberwahrenbrock et al (2013)[6]	H	33·4 (2)	66	33·8 (2·2)	66	17·2	–0·40 (–1·12 to 0·32)
Sriram et al (2012)[53]	H	43·2 (4·9)	15	42·7 (4·7)	34	2·9	0·50 (–2·44 to 3·44)
Walter et al (2012)[55]	H	44·9 (4·9)	150	43·4 (4·5)	61	9·3	1·50 (0·13 to 2·87)
Total (95% CI)			**695**		**487**	**100·0**	**0·36 (–0·17 to 0·89)**

Heterogeneity: τ^2=0·29; χ^2=15·51 to df=7 (p=0·03); I^2=55%
Test for overall effect: Z=1·35 (p=0·18)

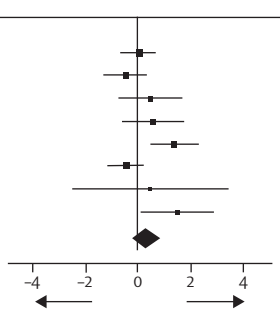

C

	Device	MSON		MSNON		Weight (%)	Mean difference* (µm; 95% CI)
		Mean (µm; SD)	Total eyes	Mean (µm; SD)	Total eyes		
INL							
Al–Louzi et al (2015)[20]	Z	64·9 (3·3)	9	64·4 (3·3)	16	2·5	0·50 (–2·19 to 3·19)
Balk et al (2014)[21]	H	42·3 (3)	144	41·5 (3)	279	49·7	0·80 (0·20 to 1·40)
Fernandes et al (2013)[27]	T	31·4 (2·7)	45	31 (2·6)	74	18·6	0·40 (–0·59 to 1·39)
Hadhoum et al (2015)[22]	H	0 (0)	50	0 (0)	20	..	Not estimable
Hokazono et al (2013)[33]	T	31·7 (2·5)	29	31·7 (2·5)	22	9·4	0·00 (–1·39 to 1·39)
Saidha et al (2015)[47]	Z	66·3 (4·6)	60	64·6 (4·4)	130	9·4	1·70 (0·31 to 3·09)
Schnurman et al (2014)[50]	H	0 (0)	33	0 (0)	25	..	Not estimable
Sriram et al (2012)[53]	H	43·2 (5)	15	43·2 (5)	15	1·4	0·00 (–3·58 to 3·58)
Walter et al (2012)[55]	H	45 (5·6)	87	44·9 (4·9)	150	9·0	0·10 (–1·31 to 1·51)
Total (95% CI)			**389**		**686**	**100·0**	**0·65 (0·23 to 1·08)**

Heterogeneity: τ^2=0·00; χ^2=4·25 to df=6 (p=0·64); I^2=0%
Test for overall effect: Z=3·01 (p=0·003)

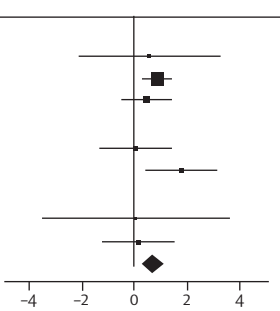

(Figure 4 continues on next page)

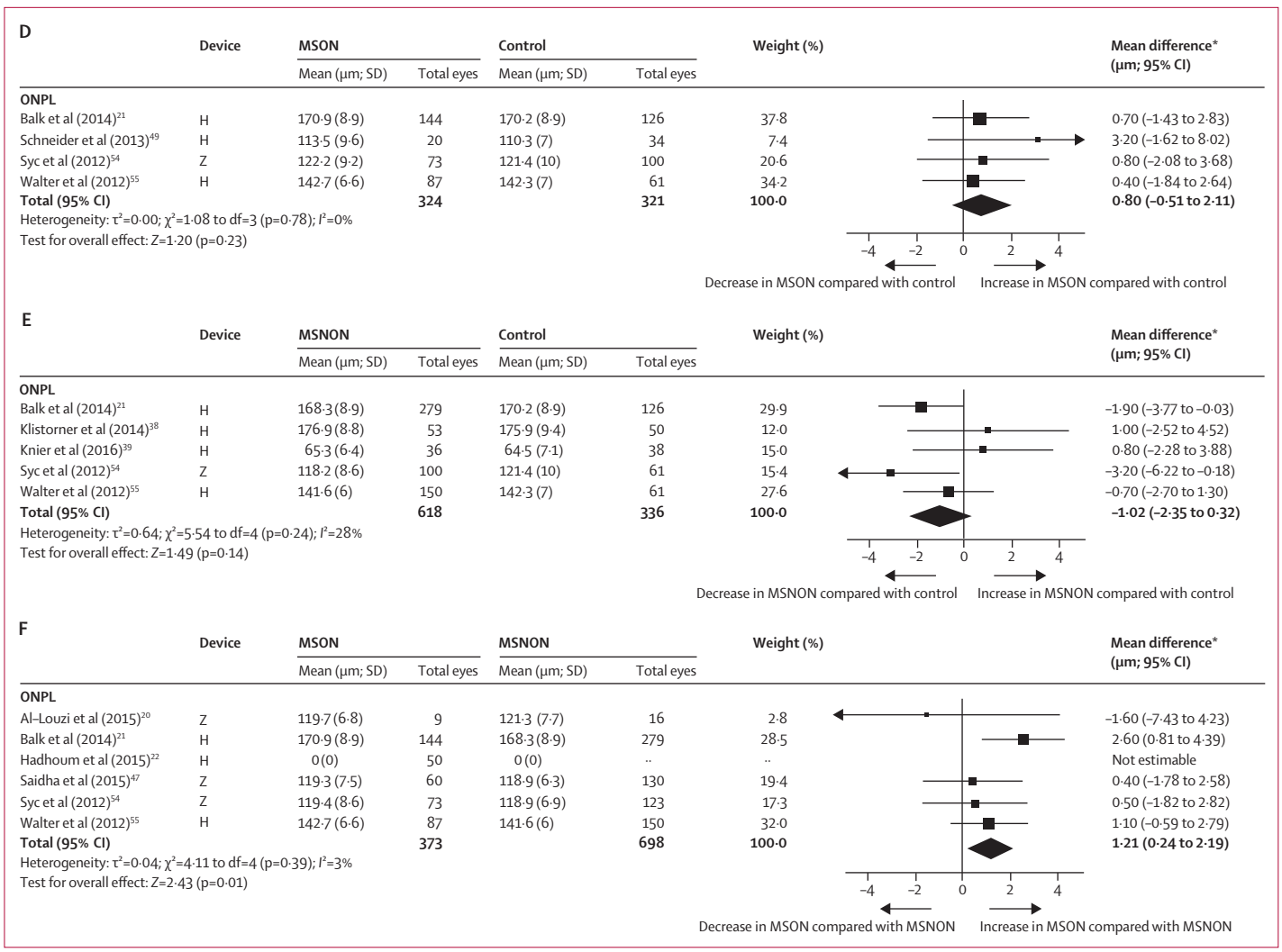

Figure 4: **Meta-analysis of macular INL SD-OCT data and ONPL SD-OCT data**
INL or ONPL data from MSON eyes (A, D) or MSNON eyes (B, E) compared with eyes from control participants, and a comparison between MSON eyes and MSNON eyes (C, F). Horizontal bar indicates 95% CI. Numbers in the total row exclude eyes for which a mean difference was not estimable. The three SD-OCT devices used are indicated as H (Spectralis, Heidelberg Engineering; Heidelberg, Germany), Z (Cirrus, Carl Zeiss Meditec; Dublin, CA, USA), and T (3D OCT-2000, Topcon Corporation; Tokyo, Japan).The appendix shows the corresponding funnel plots. INL=inner nuclear layer. SD-OCT=spectral domain optical coherence tomography. ONPL=outer nuclear layer and outer plexiform layer combined. MSON eyes=eyes with multiple-sclerosis-associated optic neuritis. MSNON eyes=eyes without multiple sclerosis optic neuritis. *Inverse variance with random effects.

prominent role for the INL.[80,82,83] Segmentation of the INL will be relevant for studies on the effect and treatment of inflammatory disease activity in multiple sclerosis. Future developments in this field are expected to include OCT angiography.[80,82,83]

Taken together, the meta-analyses suggest that the ONPL does not differ in either MSON eyes or MSNON eyes compared with control eyes. However, a small degree of ONPL thickening was apparent in MSON eyes compared with MSNON eyes, which was caused by slight thickening in MSON eyes and thinning in MSNON eyes. This outcome is consistent with published work on optic neuritis with associated multiple sclerosis, neuromyelitis optica, and anti-myelin-oligodendrocyte glycoprotein (anti-MOG) antibodies, typically during the acute phase,[11] which has been confirmed by prospective evidence for ONL thickening in anti-MOG-ON.[84] An increased MRI double-inversion recovery signal has also been associated with ONPL thickening.[32] ONPL thickening might be caused by traction, inflammation, and oedema.[20,85] The need for rigorous OCT quality control[16,86] here cannot be overemphasised because the outer retinal layers are particularly vulnerable to an easily overlooked artifact caused by placement of the measurement beam.[87,88] We anticipate that recognition of outer retinal layer volume changes will become more relevant for the differential diagnosis of optic neuritis associated with multiple sclerosis from other optic neuritis.[11,63,84,89]

A limitation to the available studies is the difficulty in obtaining retinal tissue for detailed histological

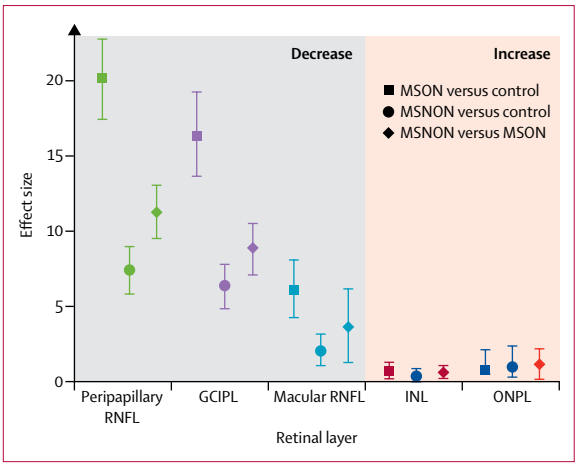

Figure 5: **Comparison of SD-OCT layer segmentation performance rating**
Head-to-head OCT layer segmentation performance based on mean effect sizes. Segmented layers shown in green (peripapillary RNFL), purple (GCIPL), and blue (macular RNFL) are significant with good effect sizes. The effect size was small for the INL and only in presence of MSON (red). Effect sizes shown in dark blue were non-significant and the shaded area indicates layers with a decrease (thinning) or increase (thickening). The effect sizes were all shown as positives to allow for a clear comparison between individual layers. The bars indicate the 95% CI. SD-OCT=spectral domain optical coherence tomography. MSON=eyes with multiple-sclerosis-associated optic neuritis. MSNON= eyes with multiple sclerosis without optic neuritis. RNFL=retinal nerve fibre layer. GCIPL=ganglion cell layer and inner plexiform layer. INL=inner nuclear layer. ONPL=outer nuclear layer and outer plexiform layer combined.

investigations.[90] A potential advantage is the availability of electrophysiological techniques.[50,91] Clinically, it is well recognised that conduction block can be caused by any structural or inflammatory lesion affecting the optic pathways. Typically these lesions are shown by MRI in the brain. Therefore, the application of MRI-based diagnostic criteria for multiple sclerosis[10] to many of the participants included in the present meta-analysis mean that contamination by retinal damage unrelated to optic neuritis is unlikely. The potential to combine OCT with pattern and multifocal electroretinogram, visual-evoked potentials and MRI provide a powerful means to assess structure and function in cohorts of homogeneous pathology.[4,11]

Will all segmented retinal layers be needed for clinical practice and trials? Probably not. A reasonable minimalistic approach will suffice, with the peripapillary RNFL assessed at least 3 months after MSON. For clinical trials and longitudinal studies on neurodegeneration, we would recommend, as a minimum, measurement of the peripapillary RNFL and macular GCIPL.[92] Studies focusing on inflammation are also advised to consider the INL. The macular RNFL is, given effect size and error bar distribution (figure 5), the least sensitive measure. However, the macular RNFL might be regarded as a backup in patients for whom imaging of the optic disc proves technically too difficult.

In summary, SD-OCT-based layer segmentation has unravelled the progression of neurodegeneration in the retina on a structural level. Atrophy affects axons and neurons of the hardwired visual pathway, that is the peripapillary RNFL, macular RNFL, and GCIPL. The INL seems to be a physiological barrier to retrograde trans-synaptic axonal degeneration. Therefore, transient INL volume changes might indicate inflammatory disease activity and response to disease-modifying treatment in multiple sclerosis, and more substantially so in optic neuritis associated with multiple sclerosis.

Contributors
AP conceived the idea for this review, did the literature search, systematic review, and meta-analysis, and wrote the first draft of the manuscript. LJBalk contributed to the literature research and statistical analyses, and revised the manuscript. LJBalc, OO, PAC, FC, TCF, EMF, EHM-L, AJG, RK, SS, PVe, PVi, and FP revised the manuscript.

Declaration of interests
AJG reports grants and other support from Inception Biosciences; grants from the National Multiple Sclerosis Society and from the US National Institutes of Health; other support from MedImmune, Mylan, Sandoz, Dr Reddy, Amneal, Momenta, Synthon, and *JAMA Neurology*, outside the submitted work; and that the Multiple Sclerosis Center, Department of Neurology, University of California San Francisco has received grant support from Novartis for participating in the OCTIMS study. AP reports that the VUmc Multiple Sclerosis Center Amsterdam participated in the OCTIMS study and the PASSOS study, which were sponsored by Novartis, and the centre has received research support for OCT projects from the Dutch Multiple Sclerosis Society. The research of AP was supported by the National Institute for Health Research (NIHR) Biomedical Research Centre based at Moorfields Eye Hospital National Health Service (NHS) Foundation Trust and University College London Institute of Ophthalmology. The views expressed are those of the authors and not necessarily those of the NHS, the NIHR, or the Department of Health. PVi has received an honorarium from Heidelberg Engineering in 2014, has received unrestricted research grants from Novartis (including for the OCTIMS study), Biogen, Genzyme, and Roche, and has participated in advisory boards for Novartis, Roche, Genzyme, and Biogen. PVi holds stocks in the following spin-off companies: Bionure Inc, Spire Bioventures, Mintlabs, and Health Engineering. TCF reports personal fees from Acorda, Novartis, and Genzyme. EMF has received speaker fees from Novartis, Acorda, Genzyme, and TEVA. SS reports grants from the University of Zurich, Clinical Research Priority Program, and Swiss Multiple Sclerosis Society, during the conduct of the study; personal fees from Bayer Healthcare, Biogen, Merck, TEVA, and Roche; and grants and personal fees from Novartis and Sanofi-Genzyme, outside the submitted work. The University Hospital of Zurich participated in the OCTIMS study, which was sponsored by Novartis. PVe received honoraria and consulting fees from Biogen, Sanofi Genzyme, Bayer, Novartis, TEVA, Merck Serono, Roche, and Almirall, and research support from Biogen, Bayer, Novartis, Sanofi Genzyme, Celegene, Sevier, and Merck Serono. EHM-L receives funding from the Instituto de Salud Carlos III, Spain, and Fondo Europeo de Desarrollo Regional (JR16/00006), Grant for Multiple Sclerosis Innovation, and Marató TV3 Charitable Foundation. EHM-L is a researcher in the OCTIMS study sponsored by Novartis; has received speaking honoraria from Biogen and Genzyme and travel reimbursement from Genzyme and Roche for international and national meetings over the past 3 years; has participated in a scientific board from Genzyme; and is a member of the working committee of International Multiple Sclerosis Visual System (IMSVISUAL) Consortium and has received non-financial support for this activity and from the Consortium. OO has received grants and personal fees from Biogen, Sanofi Genzyme, Merck Serono, Novartis, and Teva Pharmaceuticals Industries. RK reports receipt of grants from the US Department of Defense (DOD) and Veterans Affairs Office of Research and Development (VA-ORD), and the Chronic Effects of Neurotrauma Consortium: Center for the Prevention and Treatment of Visual Loss, C9251-C, Veterans Administration Rehabilitation Research Development (RRD), VA-ORD; I01

RX000889-01A1 Veterans Administration RRD, VA-ORD; 1IO1 RX002101 Veterans Administration RRD, VA-ORD; 1R01EY023279-01, National Eye Institute W81XWH-16-1-0071 DOD, CDMRP USAMRAA; and W81XWH-16-1-0211 DOD, CDMRP USAMRAA. RK reports that the University of Iowa Neuro-ophthalmology Division also participated in the Novartis-sponsored OCTIMS Study as one of the research sites and RK served on the OCTIMS Steering Committee and receives honoraria from Novartis for this activity. RK reports other support from MedFace LLC and FaceX LLC, has a patent application for assessing facial features in ophthalmological and neurological disorders pending, and has a patent application to use pupil and eye movement recordings to diagnose eye and CNS disorders, such as traumatic brain injury. PAC has received grants from Biogen-IDEC, Teva, Novartis, Annexon, and MedImmune. He has received consulting fees from Biogen-IDEC and Vertex. FP has received research support and personal compensation for activities with Alexion, Chugai, Biogen, Bayer, Merck Serono, Teva, Genzyme, Novartis, and MedImmune, is sitting on the steering committee of the MedImmune N-Momentum study and receives honoraria. FP receives funding from Deutsche Forschungsgemeinschaft, Bundesministerium für Bildung und Forschung, and Guthy Jackson Charitable Foundation. FC has received consulting fees from Clene, EMD Serono, and PRIME, and is participating as a site investigator in the Novartis-funded OCTIMS study. LJBalc reports personal fees from Biogen. LJBalk reports grants from TEVA and that the VUmc MS Center Amsterdam received financial research support for OCT projects from TEVA and participated in the OCTIMS trial, which was sponsored by Novartis.

Acknowledgments

We would like to thank Benjamin Knier, Thomas Korn, Raed Behbehani, and Elena Garcia–Martin for providing details on their published data needed for the meta-analysis.

References

1 Huang D, Swanson E, Lin C, et al. Optical coherence tomography. *Science* 1991; **254:** 1178–81.

2 Liu YZ, South FA, Xu Y, Carney PS, Boppart SA. Computational optical coherence tomography [Invited]. *Biomed Opt Express* 2017; **8:** 1549–74.

3 Petzold A, de Boer JF, Schippling S, et al. Optical coherence tomography in multiple sclerosis: a systematic review and meta-analysis. *Lancet Neurol* 2010; **9:** 921–32.

4 Balcer LJ, Miller DH, Reingold SC, Cohen JA. Vision and vision-related outcome measures in multiple sclerosis. *Brain* 2014; **138:** 11–27.

5 Gabilondo I, Martnez-Lapiscina EH, Martnez-Heras E, et al. Trans-synaptic axonal degeneration in the visual pathway in multiple sclerosis. *Ann Neurol* 2014; **75:** 98–107.

6 Oberwahrenbrock T, Ringelstein M, Jentschke S, et al. Retinal ganglion cell and inner plexiform layer thinning in clinically isolated syndrome. *Mult Scler* 2013; **19:** 1887–95.

7 Costello F. The afferent visual pathway: designing a structural-functional paradigm of multiple sclerosis. *ISRN Neurol* 2013; **2013:** 134858.

8 Graham SL, Klistorner A. Afferent visual pathways in multiple sclerosis: a review. *Clin Experiment Ophthalmol* 2017; **45:** 62–72.

9 Cruz-Herranz A, Balk LJ, Oberwahrenbrock T, et al. The APOSTEL recommendations for reporting quantitative optical coherence tomography studies. *Neurology* 2016; **86:** 2303–09.

10 Polman CH, Reingold SC, Banwell B, et al. Diagnostic criteria for multiple sclerosis: 2010 revisions to the McDonald criteria. *Ann Neurol* 2011; **69:** 292–302.

11 Petzold A, Wattjes MP, Costello F, et al. The investigation of acute optic neuritis: a review and proposed protocol. *Nat Rev Neurol* 2014; **10:** 447–58.

12 Voss E, Raab P, Trebst C, Stangel M. Clinical approach to optic neuritis: pitfalls, red flags and differential diagnosis. *Ther Adv Neurol Disord* 2011; **4:** 123–34.

13 Beck R. The clinical profile of optic neuritis-experience of the optic neuritis treatment trial. *Arch Ophthalmol* 1991; **109:** 1673–78.

14 Costello F, Pan YI, Yeh EA, Hodge W, Burton JM, Kardon R. The temporal evolution of structural and functional measures after acute optic neuritis. *J Neurol Neurosurg Psychiatry* 2015; **86:** 1369–73.

15 Lublin FD, Reingold SC, Cohen JA, et al. Defining the clinical course of multiple sclerosis: the 2013 revisions. *Neurology* 2014; **83:** 278–86.

16 Tewarie P, Balk L, Costello F, et al. The OSCAR-IB consensus criteria for Retinal OCT quality assessment. *PLoS One* 2012; **7:** e34823.

17 Schippling S, Balk L, Costello F, et al. Quality control for retinal OCT in multiple sclerosis: validation of the OSCAR-IB criteria. *Mult Scler* 2015; **21:** 163–70.

18 Review Manager (RevMan) [Computer program]. Version 5.3. Copenhagen: The Nordic Cochrane Centre, The Cochrane Collaboration, 2014.

19 Kiernan DF, Mieler WF, ad Hariprasad SM. Spectral-domain optical coherence tomography: a comparison of modern high-resolution retinal imaging systems. *Am J Ophthalmol* 2010; **149:** 18–31.

20 Al-Louzi OA, Bhargava P, Newsome SD, et al. Outer retinal changes following acute optic neuritis. *Mult Scler* 2016; **22:** 362–72.

21 Balk LJ, Twisk JWR, Steenwijk MD, et al. A dam for retrograde axonal degeneration in multiple sclerosis? *J Neurol Neurosurg Psychiatry* 2014; **85:** 782–89.

22 Behbehani R, Al-Hassan AA, Al-Khars A, Sriraman D, Alroughani R. Retinal nerve fiber layer thickness and neurologic disability in relapsing-remitting multiple sclerosis. *J Neurol Sci* 2015; **359:** 305–08.

23 Behbehani R, Al-Moosa A, Sriraman D, Alroughani R. Ganglion cell analysis in acute optic neuritis. *Mult Scler Relat Disord* 2016; **5:** 66–69.

24 Chilinska A, Ejma M, Turno-Krecicka A, Guranski K, Misiuk-Hojlo M. Analysis of retinal nerve fibre layer, visual evoked potentials and relative afferent pupillary defect in multiple sclerosis patients. *Clin Neurophysiol* 2016; **127:** 821–26.

25 Esen E, Sizmaz S, Balal M, et al. Evaluation of the innermost retinal layers and visual evoked potentials in patients with multiple sclerosis. *Curr Eye Res* 2016; **41:** 1353–58.

26 Feng L, Shen J, Jin X, Li J, Li Y. The evaluation of the retinal nerve fiber layer in multiple sclerosis with special-domain optical coherence tomography. *Ophthalmologica* 2013; **230:** 116–20.

27 Fernandes DB, Raza AS, Nogueira RGF, et al. Evaluation of inner retinal layers in patients with multiple sclerosis or neuromyelitis optica using optical coherence tomography. *Ophthalmology* 2013; **120:** 387–94.

28 Fjeldstad C, Bemben M, Pardo G. Reduced retinal nerve fiber layer and macular thickness in patients with multiple sclerosis with no history of optic neuritis identified by the use of spectral domain high-definition optical coherence tomography. *J Clin Neurosci* 2011; **18:** 1469–72.

29 Garcia-Martin E, Pablo LE, Herrero R, et al. Neural networks to identify multiple sclerosis with optical coherence tomography. *Acta Ophthalmol* 2013; **91:** e628–34.

30 Gelfand JM, Goodin DS, Boscardin WJ, Nolan R, Cuneo A, Green AJ. Retinal axonal loss begins early in the course of multiple sclerosis and is similar between progressive phenotypes. *PLoS One* 2012; **7:** e36847.

31 González-López JJ, Rebolleda G, Leal M, et al. Comparative diagnostic accuracy of ganglion cell-inner plexiform and retinal nerve fiber layer thickness measures by Cirrus and Spectralis optical coherence tomography in relapsing-remitting multiple sclerosis. *Biomed Res Int* 2014; **2014:** 128517.

32 Hadhoum N, Hodel J, Defoort-Dhellemmes S, et al. Length of optic nerve double inversion recovery hypersignal is associated with retinal axonal loss. *Mult Scler* 2015; **22:** 649–58.

33 Hokazono K, Raza AS, Oyamada MK, Hood DC, Monteiro ML. Pattern electroretinogram in neuromyelitis optica and multiple sclerosis with or without optic neuritis and its correlation with FD-OCT and perimetry. *Doc Ophthalmol* 2013; **127:** 201–15.

34 Huang-Link YM, Fredrikson M, Link H. Benign multiple sclerosis is associated with reduced thinning of the retinal nerve fiber and ganglion cell layers in non-optic-neuritis eyes. *J Clin Neurol* 2015; **11:** 241–47.

35 Kaushik M, Wang CY, Barnett MH, et al. Inner nuclear layer thickening is inversley proportional to retinal ganglion cell loss in optic neuritis. *PLoS One* 2013; **8:** e78341.

36 Khalil DH, Said MM, Abdelhakim MASE, Labeeb DM. OCT and visual field changes as useful markers for follow-up of axonal loss in multiple sclerosis in Egyptian patients. *Ocul Immunol Inflamm* 2017; **25:** 315–22.

37 Khanifar AA, Parlitsis GJ, Ehrlich JR, et al. Retinal nerve fiber layer evaluation in multiple sclerosis with spectral domain optical coherence tomography. *Clin Ophthalmol* 2010; **4:** 1007–13.

38 Klistorner A, Sriram P, Vootakuru N, et al. Axonal loss of retinal neurons in multiple sclerosis associated with optic radiation lesions. *Neurology* 2014; **82:** 2165–72.

39 Knier B, Berthele A, Buck D, et al. Optical coherence tomography indicates disease activity prior to clinical onset of central nervous system demyelination. *Mult Scler* 2016; **22:** 893–900.

40 Lange AP, Zhu F, Sayao AL, et al. Retinal nerve fiber layer thickness in benign multiple sclerosis. *Mult Scler* 2013; **19:** 1275–81.

41 Modvig S, Degn M, Sander B, et al. Cerebrospinal fluid neurofilament light chain levels predict visual outcome after optic neuritis. *Mult Scler* 2016; **22:** 590–98.

42 Narayanan D, Cheng H, Bonem KN, Saenz R, Tang RA, Frishman LJ. Tracking changes over time in retinal nerve fiber layer and ganglion cell-inner plexiform layer thickness in multiple sclerosis. *Mult Scler* 2014; **20:** 1331–41.

43 Oberwahrenbrock T, Schippling S, Ringelstein M, et al. Retinal damage in multiple sclerosis disease subtypes measured by high-resolution optical coherence tomography. *Mult Scler Int* 2012; **2012:** 530305.

44 Park KA, Kim J, Oh SY. Analysis of spectral domain optical coherence tomography measurements in optic neuritis: differences in neuromyelitis optica, multiple sclerosis, isolated optic neuritis and normal healthy controls. *Acta Ophthalmol* 2014; **92:** e57–65.

45 Petracca M, Cordano C, Cellerino M, et al. Retinal degeneration in primary-progressive multiple sclerosis: a role for cortical lesions? *Mult Scler* 2016; **23:** 43–50.

46 Rebolleda G, Garca-Garca A, Won Kim HR, Muñoz-Negrete FJ. Comparison of retinal nerve fiber layer measured by time domain and spectral domain optical coherence tomography in optic neuritis. *Eye* 2011; **25:** 233–38.

47 Saidha S, Al-Louzi O, Ratchford JN, et al. Optical coherence tomography reflects brain atrophy in multiple sclerosis: a four-year study. *Ann Neurol* 2015; **78:** 801–13.

48 Salari M, Janghorbani M, Etemadifar M, Dehghani A, Razmjoo H, Naderian G. Effects of vitamin D on retinal nerve fiber layer in vitamin D deficient patients with optic neuritis: Preliminary findings of a randomized, placebo-controlled trial. *J Res Med Sci* 2015; **20:** 372–78.

49 Schneider E, Zimmermann H, Oberwahrenbrock T, et al. Optical coherence tomography reveals distinct patterns of retinal damage in neuromyelitis optica and multiple sclerosis. *PLoS One* 2013; **8:** e66151.

50 Schnurman ZS, Frohman TC, Beh SC, et al. Retinal architecture and mfERG Optic nerve head component response characteristics in MS. *Neurology* 2014; **82:** 1888–96.

51 Soufi G, AitBenhaddou E, Hajji Z, et al. Evaluation of retinal nerve fiber layer thickness measured by optical coherence tomography in Moroccan patients with multiple sclerosis. *J Fr Ophtalmol* 2015; **38:** 497–503.

52 Sriram P, Wang C, Yiannikas C, et al. Relationship between optical coherence tomography and electrophysiology of the visual pathway in non-optic neuritis eyes of multiple sclerosis patients. *PLoS One* 2014; **9:** e102546.

53 Sriram P, Graham SL, Wang C, Yiannikas C, Garrick R, Klistorner A. Trans-synaptic retinal degeneration in optic neuropathies: optical coherence tomography study. *Invest Ophthalmol Vis Sci* 2012; **53:** 1271–75.

54 Syc SB, Saidha S, Newsome SD, et al. Optical coherence tomography segmentation reveals ganglion cell layer pathology after optic neuritis. *Brain* 2012; **135:** 521–33.

55 Walter SD, Ishikawa H, Galetta KM, et al. Ganglion cell loss in relation to visual disability in multiple sclerosis. *Ophthalmology* 2012; **119:** 1250–57.

56 Xu LT, Bermel RA, Nowacki AS, Kaiser PK. Optical coherence tomography for the detection of remote optic neuritis in multiple sclerosis. *J Neuroimaging* 2016; **26:** 283–88.

57 Zimmermann H, Freing A, Kaufhold F, et al. Optic neuritis interferes with optical coherence tomography and magnetic resonance imaging correlations. *Mult Scler* 2013; **19:** 443–50.

58 Bailar JC. The promise and problems of meta-analysis. *N Eng J Med* 1997; **337:** 559–61.

59 Greenland S. Can meta-analysis be salvaged? *Am J Epidemiol* 1994; **140:** 783–87.

60 Frohman E, Costello F, Zivadinov R, et al. Optical coherence tomography in multiple sclerosis. *Lancet Neurol* 2006; **5:** 853–63.

61 Warner CV, Syc SB, Stankiewicz AM, et al. The impact of utilizing different optical coherence tomography devices for clinical purposes and in multiple sclerosis trials. *PLoS One* 2011; **6:** e22947.

62 Masland RH. The fundamental plan of the retina. *Nat Neurosci* 2001; **4:** 877–86.

63 Petzold A, Wong S, Plant GT. Autoimmunity in visual loss. *Handb Clin Neurol* 2016; **133:** 353–76.

64 Dinkin M. Trans-synaptic retrograde degeneration in the human visual system: slow, silent, and real. *Curr Neurol Neurosci Rep* 2017; **17:** 16.

65 Balk LJ, Cruz-Herranz A, Albrecht P, et al. Timing of retinal neuronal and axonal loss in MS: a longitudinal OCT study. *J Neurol* 2016; **263:** 1323–31.

66 Graham EC, You Y, Yiannikas C, et al. Progressive loss of retinal ganglion cells and axons in nonoptic neuritis eyes in multiple sclerosis: a longitudinal optical coherence tomography study. *Invest Ophthalmol Vis Sci* 2016; **57:** 2311–17.

67 Talman LS, Bisker ER, Sackel DJ, et al. Longitudinal study of vision and retinal nerve fiber layer thickness in multiple sclerosis. *Ann Neurol* 2010; **67:** 749–60.

68 Serbecic N, Aboul-Enein F, Beutelspacher SC, et al. High resolution spectral domain optical coherence tomography (SD-OCT) in multiple sclerosis: the first follow up study over two years. *PLoS One* 2011; **6:** e19843.

69 Knier B, Schmidt P, Aly L, et al. Retinal inner nuclear layer volume reflects response to immunotherapy in multiple sclerosis. *Brain* 2016; **139:** 2855–63.

70 Saidha S, Sotirchos ES, Ibrahim MA, et al. Microcystic macular oedema, thickness of the inner nuclear layer of the retina, and disease characteristics in multiple sclerosis: a retrospective study. *Lancet Neurol* 2012; **11:** 963–72.

71 Sepulcre J, Murie-Fernandez M, Salinas-Alaman A, García-Layana A, Bejarano B, Villoslada P. Diagnostic accuracy of retinal abnormalities in predicting disease activity in MS. *Neurology* 2007; **68:** 1488–94.

72 Petzold A, Nijland PG, Balk LJ, et al. Visual pathway neurodegeneration winged by mitochondrial dysfunction. *Ann Clin Transl Neurol* 2015; **2:** 140–50.

73 Mahad DJ, Ziabreva I, Campbell G, et al. Mitochondrial changes within axons in multiple sclerosis. *Brain* 2009; **132:** 1161–74.

74 Cadavid D, Balcer L, Galetta S, et al, for the RENEW Study Investigators. Safety and efficacy of opicinumab in acute optic neuritis (RENEW): a randomised, placebo-controlled, phase 2 trial. *Lancet Neurol* 2017; **16:** 189–99.

75 Kupersmith MJ, Garvin MK, Wang JK, Durbin M, Kardon R. Retinal ganglion cell layer thinning within one month of presentation for optic neuritis. *Mult Scler* 2016; **22:** 641–48.

76 Gabilondo I, Martnez-Lapiscina EH, Fraga-Pumar E, et al. Dynamics of retinal injury after acute optic neuritis. *Ann Neurol* 2015; **77:** 517–28.

77 Britze J, Pihl-Jensen G, Frederiksen JL. Retinal ganglion cell analysis in multiple sclerosis and optic neuritis: a systematic review and meta-analysis. *J Neurol* 2017; published online May 31. DOI:10.1007/s00415-017-8531-y.

78 Burggraaff MC, Trieu J, de Vries-Knoppert WA, Balk L, Petzold A. The clinical spectrum of microcystic macular edema. *Invest Ophthalmol Vis Sci* 2014; **55:** 952–61.

79 Brandt AU, Oberwahrenbrock T, Kadas EM, Lagrèze WA, Paul F. Dynamic formation of macular microcysts independent of vitreous traction changes. *Neurology* 2014; **83:** 73–77.

80 Petzold A. Retinal glymphatic system: an explanation for transient retinal layer volume changes? *Brain* 2016; **139:** 2816–19.

81 Gelfand JM, Nolan R, Schwartz DM, Graves J, Green AJ. Microcystic macular oedema in multiple sclerosis is associated with disease severity. *Brain* 2012; **135:** 1786–93.

82 Spaide RF. Retinal vascular cystoid macular edema: review and new theory. *Retina* 2016; **36:** 1823–42.

83 Wostyn P, De Groot V, Van Dam D, Audenaert K, Killer HE, De Deyn PP. Age-related macular degeneration, glaucoma and Alzheimer's disease: amyloidogenic diseases with the same glymphatic background? *Cell Mol Life Sci* 2016; **73:** 4299–301.

84 Havla J, Kümpfel T, Schinner R, et al. Myelin-oligodendrocyte-glycoprotein (MOG) autoantibodies as potential markers of severe optic neuritis and subclinical retinal axonal degeneration. *J Neurol* 2017; **264:** 139–51.

85 Petzold A, Plant GT. Clinical use of OCT and MSON mimics. In: Petzold A, ed. Optical Coherence tomography in multiple sclerosis. London: Springer, 2016: 59–83.

86 Schlaeger R, Papinutto N, Panara V, et al. Spinal cord gray matter atrophy correlates with multiple sclerosis disability. *Ann Neurol* 2014; **76:** 568–80.

87 Balk LJ, de Vries-Knoppert WA, Petzold A. A simple sign for recognizing off-axis OCT measurement beam placement in the context of multicentre studies. *PLoS One* 2012; **7:** e48222.

88 Oberwahrenbrock T, Weinhold M, Mikolajczak J, et al. Reliability of intra-retinal layer thickness estimates. *PLoS One* 2015; **10:** e0137316.

89 Martinez-Lapiscina EH, Sepulveda M, Torres-Torres R, et al. Usefulness of optical coherence tomography to distinguish optic neuritis associated with AQP4 or MOG in neuromyelitis optica spectrum disorders. *Ther Adv Neurol Disord* 2016; **9:** 436.

90 Green AJ, McQuaid S, Hauser SL, Allen IV, Lyness R. Ocular pathology in multiple sclerosis: retinal atrophy and inflammation irrespective of disease duration. *Brain* 2010; **133:** 1591–601.

91 Holder GE. Pattern electroretinography (PERG) and an integrated approach to visual pathway diagnosis. *Prog Retin Eye Res* 2001; **20:** 531–61.

92 Petzold A. Neuroprotection and visual function after optic neuritis. *Curr Opin Neurol* 2017; **30:** 67–73.